SAND2012-5973C

Deformation and Delamination in Polymer Metal Thin Film Structures

N. R. Moody
E. D. Reedy, E. Corona, D. P. Adams, R. W. Friddle,
M. S. Kennedy, M. J. Cordill, D. F. Bahr

Sandia National Laboratories, Livermore, CA, USA
Sandia National Laboratories, Albuquerque, NM, USA
Clemson University, Clemson, SC, USA
Erich Schmid Institute, Leoben, Austria
Washington State University, Pullman, WA, USA

Symposium on Thin Films on Compliant Substrates
ICMCTF
San Diego, CA
April 23-27, 2012

Many Sandia programs incorporate thin metal, ceramic and polymer films where performance and reliability must be assured.

MEMS mirrors

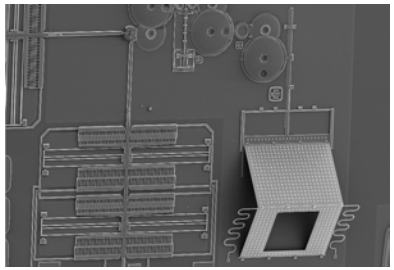

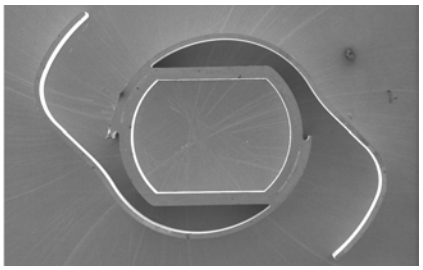

Micro springs

microelectronics

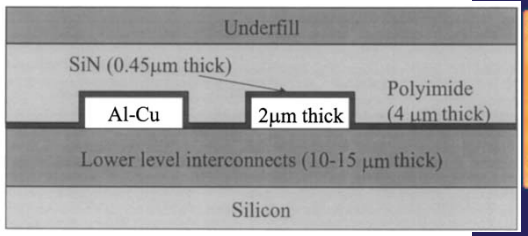

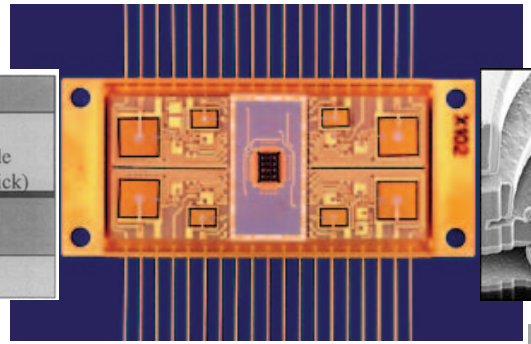

protective coatings

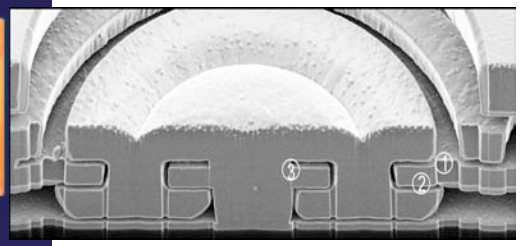

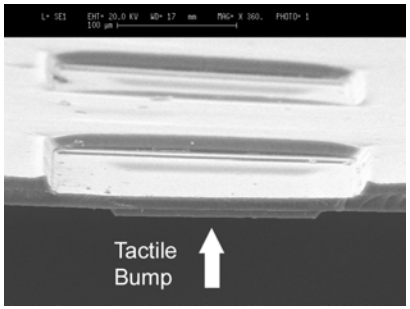

Tactile Sensor

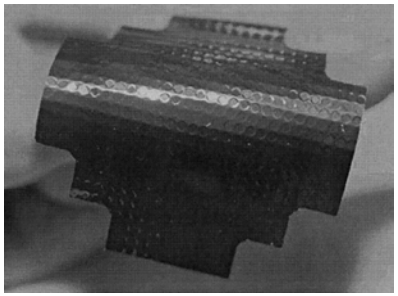

Flexible Skin

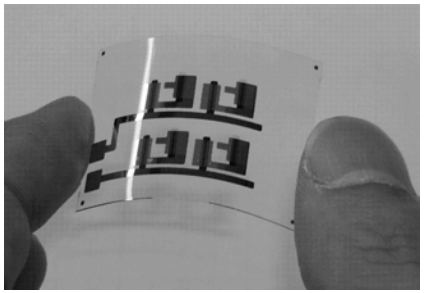

Flexible Electronics

Layers of dissimilar materials leads to high stresses across the interfaces.

Thin films are typically subject to appreciable residual stress that can trigger deformation and fracture.

Compressive stresses can lead to wrinkling, delamination, and buckling.

wrinkling

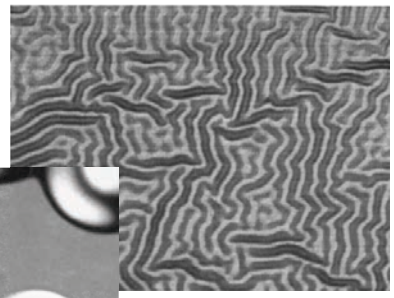

buckling

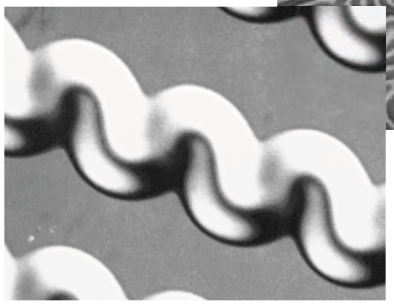

(Lacour 2003)

(Moody 2001)

delamination

Tensile stresses can lead to film fracture and decohesion.

mudflat cracking

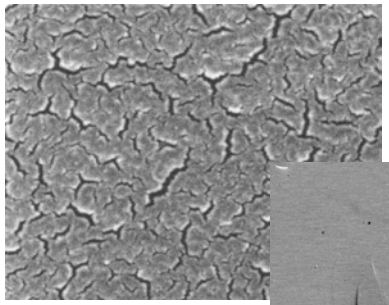

channel cracking

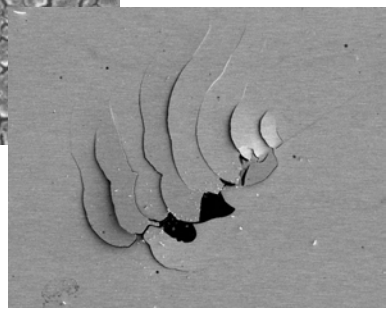

(Lacour 2003)

(Moody 2004)

decohesion

Adhesion and fracture are critical issues

These are the same issues we face in assuring performance of polymer-metal interfaces in coated wires and flexible sheets.

Polyimide coated copper wires exhibit multiple failure modes when embedded in an epoxy fiberglass layup.

High stress, humidity, and diffusion can alter composition, structure, properties, adhesion, and toughness leading to premature failure.

Quad Layer Copper Wire

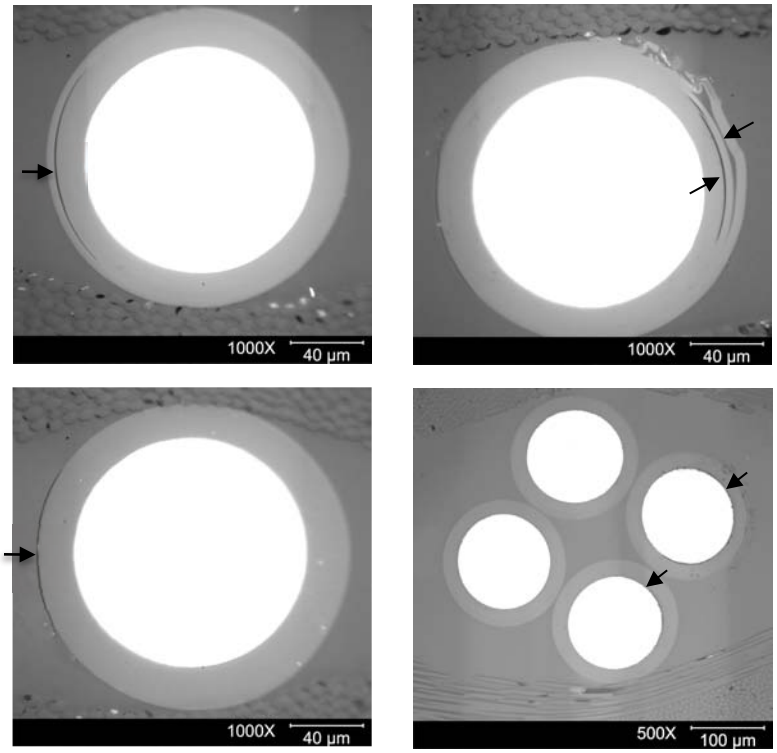

Variability in stresses, multiple fracture modes, and undefined processes prevent assessing reliability and predicting service life.

Adhesion is defined as the total irreversible energy per unit area required to separate materials at the interface.

.

True work of adhesion is the energy required to create free surfaces

$$W_A = \gamma_f + \gamma_s - \gamma_{fs}$$

It is often determined by contact angle measurements

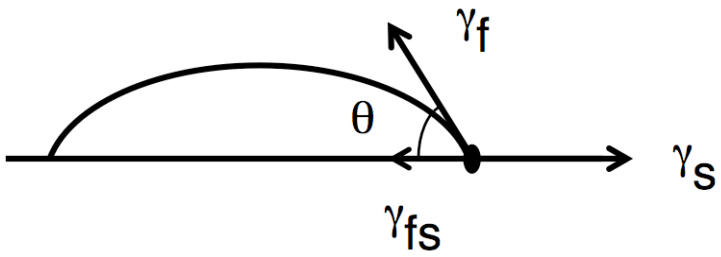

$$\gamma_{fs} = \gamma_s - \gamma_f \cos\theta$$

$$W_A = \gamma_f + \gamma_s - \gamma_{fs} = \gamma_f(1 - \cos\theta)$$

Practical work of adhesion measured by delamination

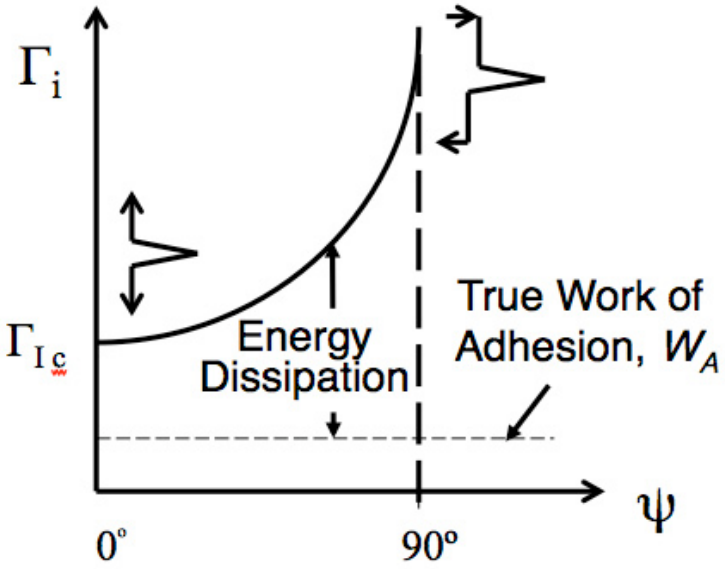

Often includes energies from additional processes

Conical tip indentation triggered delamination along the 5.5 μm thick PMMA-Substrate interface.

.

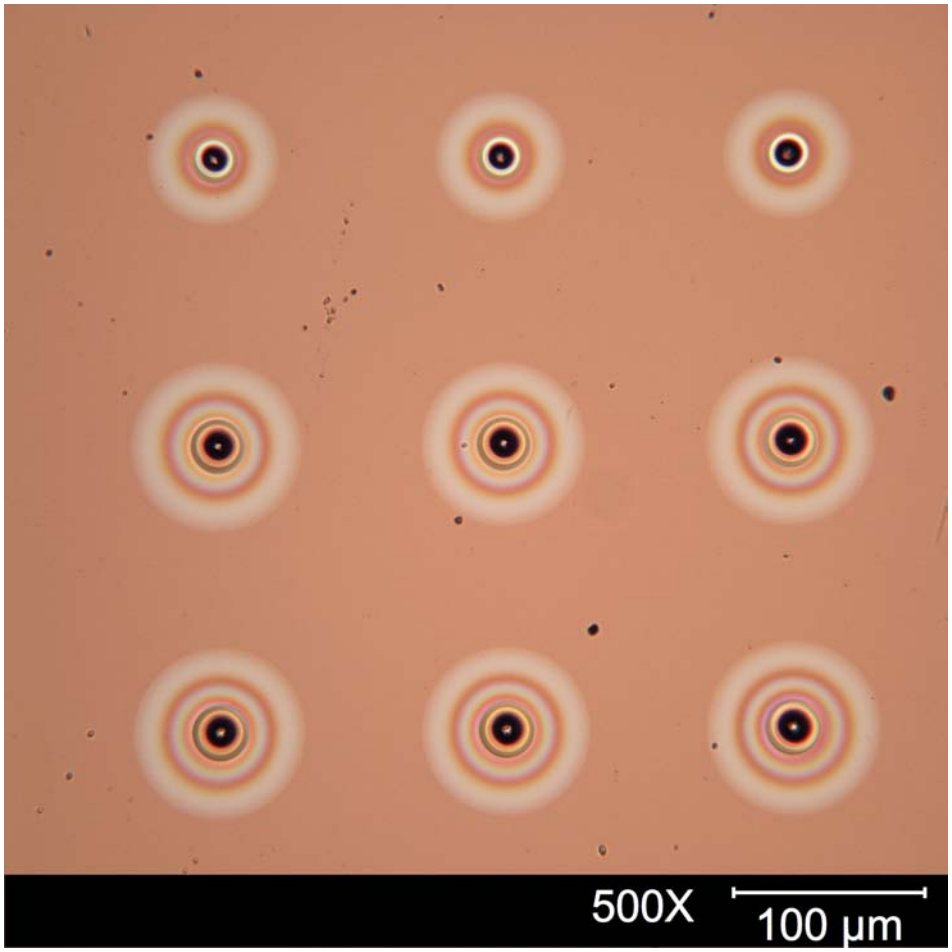

Fracture energies for indentation induced blisters can be determined using models for circular blister formation.

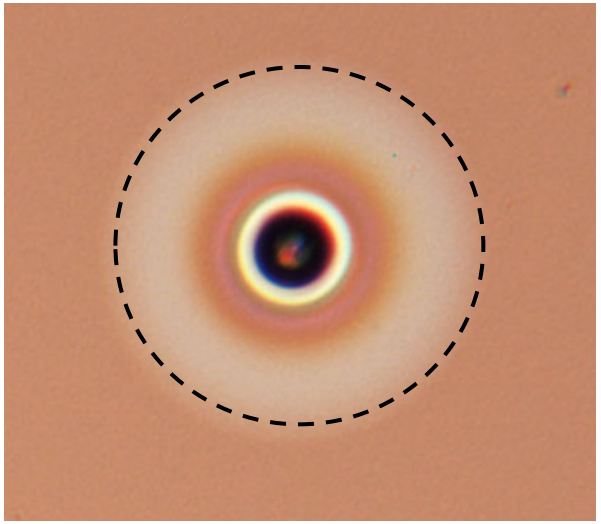

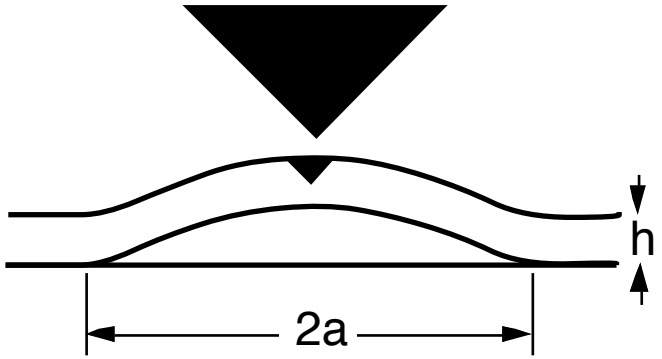

The stress for delamination is given by,

$$\sigma_a = \frac{\mu E}{12\left(1-\nu^2\right)}\left(\frac{h}{a}\right)^2$$

stress from indentation,

$$\sigma_V = \frac{EV}{2\pi(1-\nu)a^2h}$$

The fracture energy follows,

$$G(\psi) = \frac{\left(1-\nu^2\right)h\sigma_V^2}{2E} + (1-\alpha)\frac{(1-\nu)h\sigma_r^2}{E} - (1-\alpha)\frac{\left(1-\nu^2\right)\left(\sigma_V-\sigma_a\right)^2}{\sigma_V^2 E}$$

Marshall and Evans (1984)

Hutchinson and Suo (1992)

Fracture energies for indentation induced blisters can be determined using models for circular blister formation.

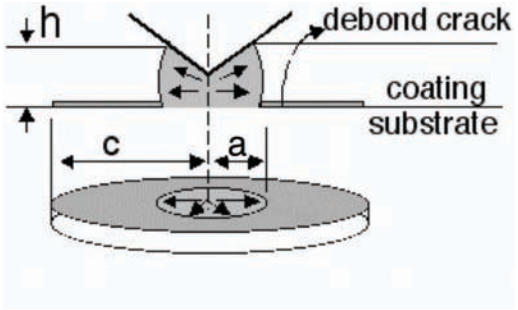

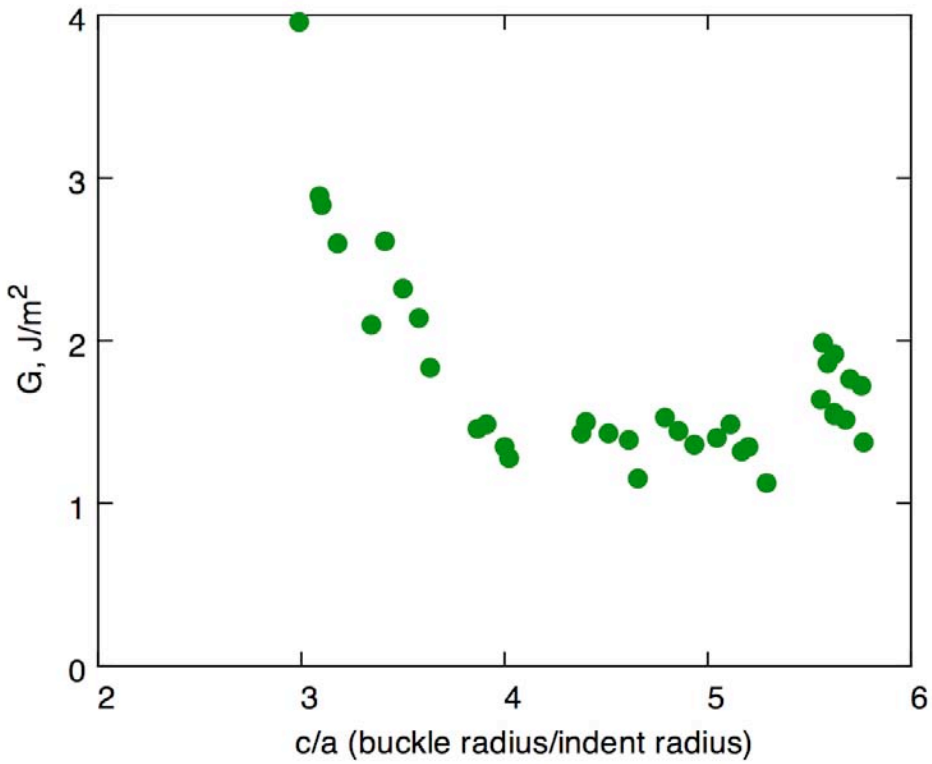

Analysis provides a value for G, but extensive deformation masks true works of adhesion and underlying mechanisms.

Purpose

Characterize deformation and fracture in model hard film on compliant substrate systems

Tasks

Employed model film systems to isolate effects of compliance and minimize deformation by dislocations

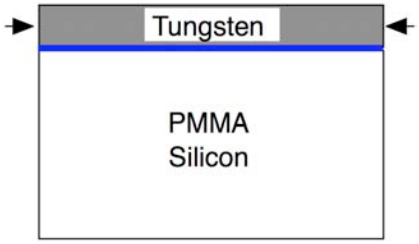

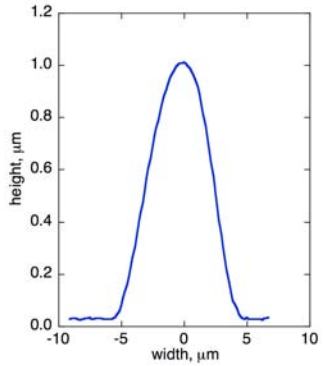

Used optical and atomic force microscopy to characterize film buckling and substrate deformation.

Determined interfacial fracture energies from buckle heights and widths and models describing effects of substrate compliance and deformation on fracture

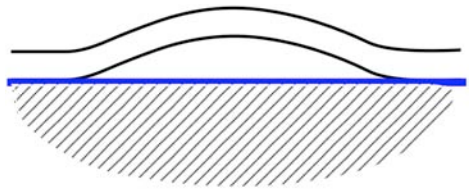

The stressed overlayer approach was used to study failure of highly stressed hard metal films on thick polymer substrates.

.

100W/PMMA

200W/PMMA

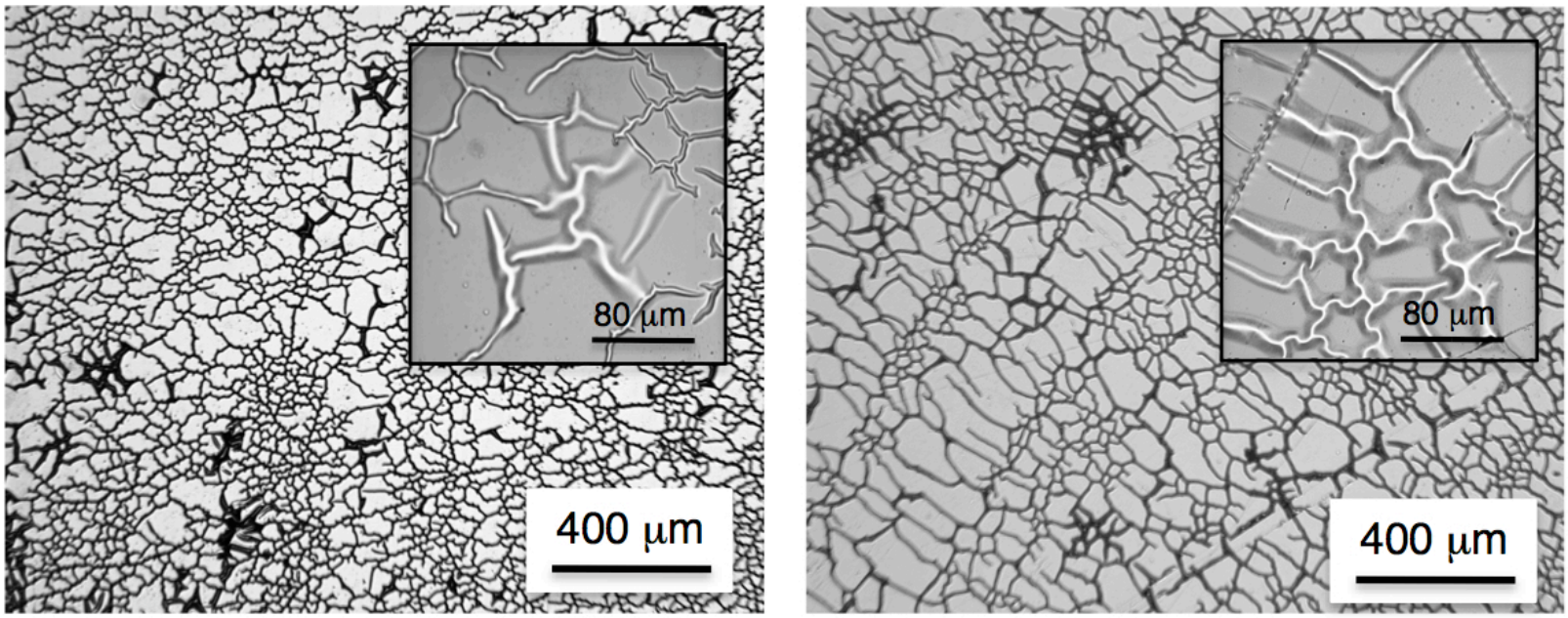

Small buckles formed spontaneously following film deposition forming a dense ring-like network interspersed with regions of large buckles

Mechanics-based modeling gives us the stresses and fracture energies for adhesive film failure of compressively stressed films

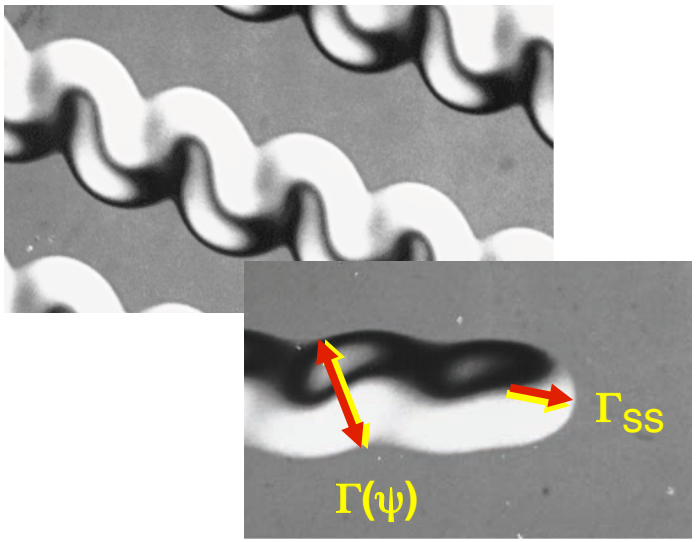

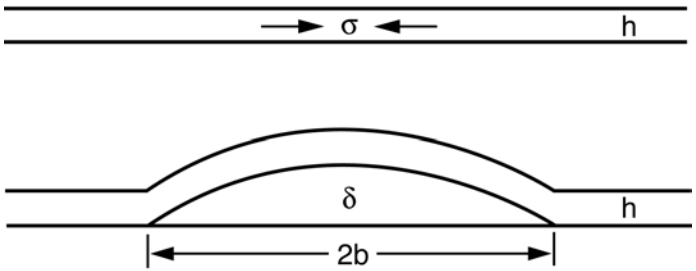

The stress for delamination is,

$$\sigma_b = \frac{\pi^2}{12}\frac{E}{(1-\nu^2)}\left(\frac{h}{b}\right)^2$$

Residual stress is as follows,

$$\sigma_r = \sigma_b\left[\frac{3}{4}\left(\frac{\delta^2}{h^2}+1\right)\right]$$

The strain energy released along the side wall is given by,

$$\Gamma(\psi) = \left[\frac{(1-\nu^2)h}{2E}\right](\sigma_r-\sigma_b)(\sigma_r+3\sigma_b)$$

and along the propagating curved front.

$$\Gamma_{ss} = \left[\frac{(1-\nu^2)h\sigma_r^2}{2E}\right]\left(1-\frac{\sigma_b}{\sigma_r}\right)^2$$

Hutchinson and Suo (1992)

The analysis is valid for hard elastic films on rigid elastic substrates.

Yu and Hutchinson used a two part approach treating the buckled portion of the film separately from the remaining film/substrate system

.

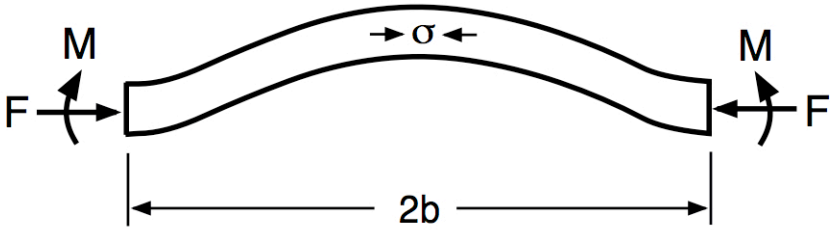

The buckled portion of the film was modeled using von Karmen nonlinear plate theory

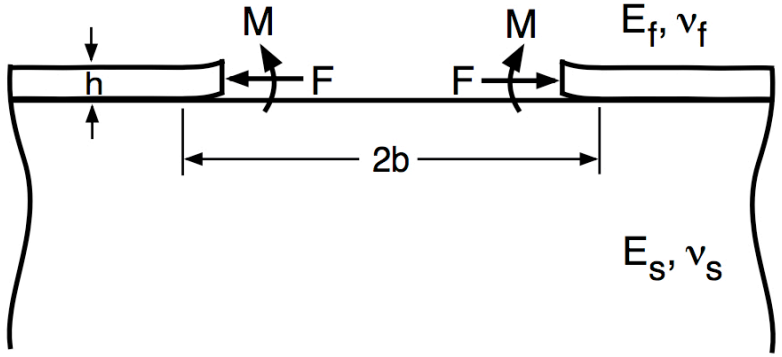

The film/substrate system is a linear plane strain problem solved using an integral equation formulation

The solutions were matched at the detached edges of the film by requiring continuity of displacements and rotations.

Substrate compliance increases the fracture energy for adhesive film failure of compressively stressed films

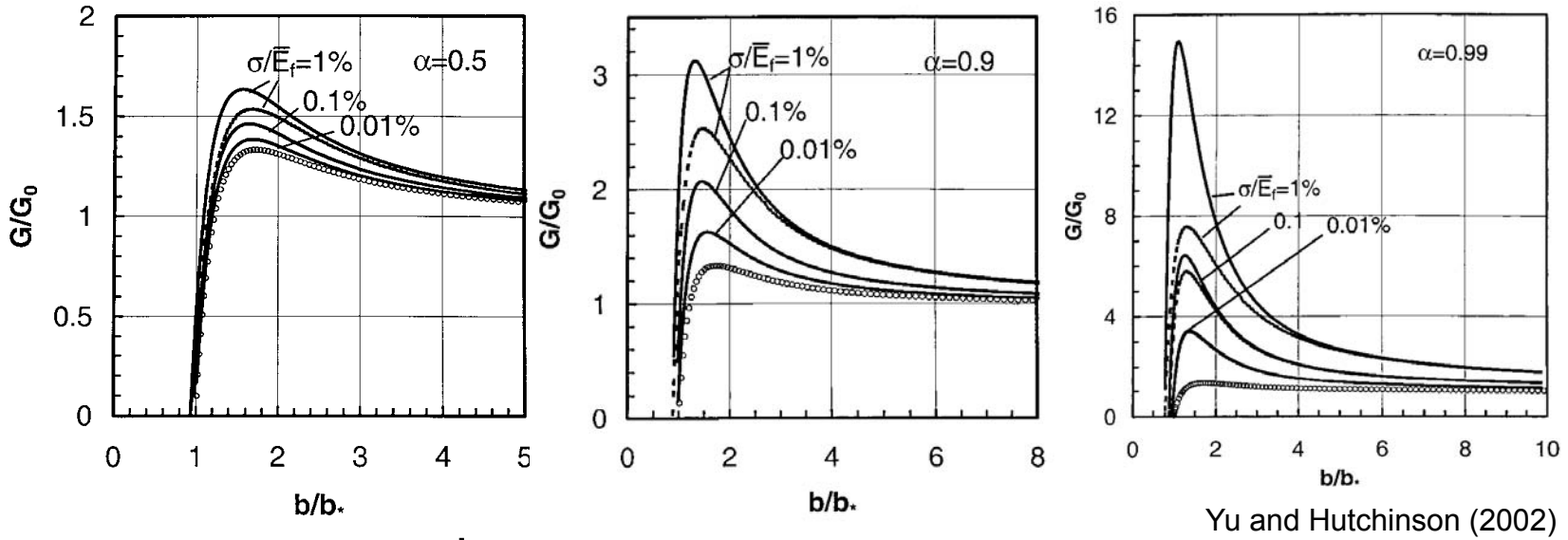

Yu and Hutchinson (2002)

α and β are the Dundar's parameters

Go is given by,

$$G_o = \left(\frac{1}{2}\right)\frac{\sigma^2 h\left(1-\nu^2\right)}{E_f}$$

$$\frac{b}{b_*} = \sqrt{\frac{\sigma}{\sigma_*}}$$

$$b_* = \frac{\pi h}{2\sqrt{3}}\sqrt{\frac{E_f}{(1-\nu^2)\sigma}};\sigma_* = \frac{\pi^2 E_f}{12(1-\nu^2)}\left(\frac{h}{b}\right)^2$$

W/Si α=0.44

W/SiO2 α=0.71

Si/PMMA α=0.95

W/PMMA α=0.985

$$\frac{\sigma}{\bar{E}_f} = 0.004$$

b,h determined using AFM

σ = -1.7 GPa from wafer curvature

Cohesive Zone finite element simulations were used to define the effects of substrate compliance on buckle-driven delamination

Material separation defined using a cohesive zone model

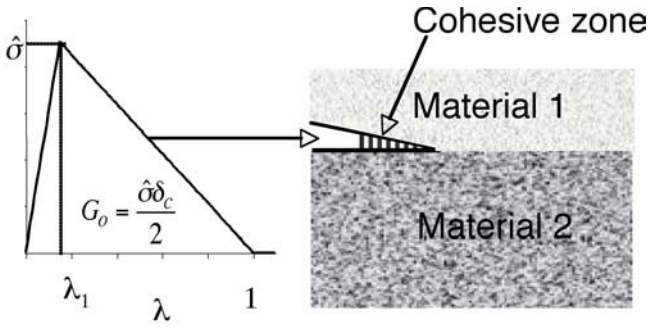

Effective Separation $\lambda = \sqrt{\left(\frac{\delta_n}{\delta_n^c}\right)^2 + \left(\frac{\delta_t}{\delta_t^c}\right)^2}$

- Key parameters are:
  - specified traction-separation
  - cohesive strength $\hat{\sigma}$
  - work of separation/unit area G_o.
- Failure modeled as a gradual process with tractions resisting separation

Cohesive zone elements were inserted along the initial 50 μm of interface

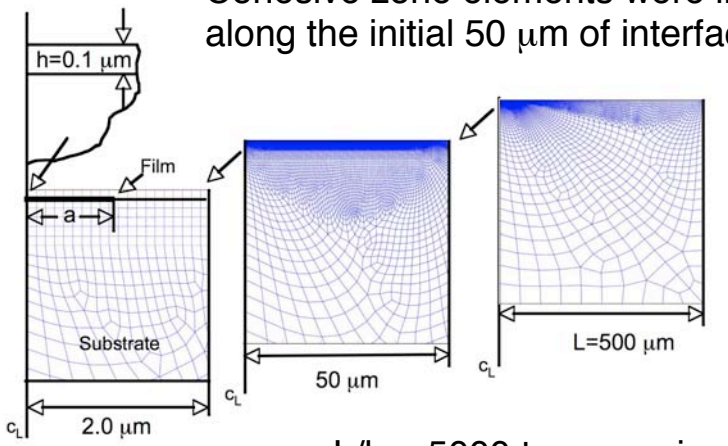

L/h = 5000 to approximate infinite substrate

- Film modeled with a single layer of elements
- Cohesive zone elements along the interface to model buckle-driven delamination
- Highly refined submesh to capture large region of nonuniform deformation

Substrate compliance markedly increases the fracture energy for film failure over values calculated using a rigid substrate analysis

Prescribe thickness, properties, stress, and interfacial toughness.

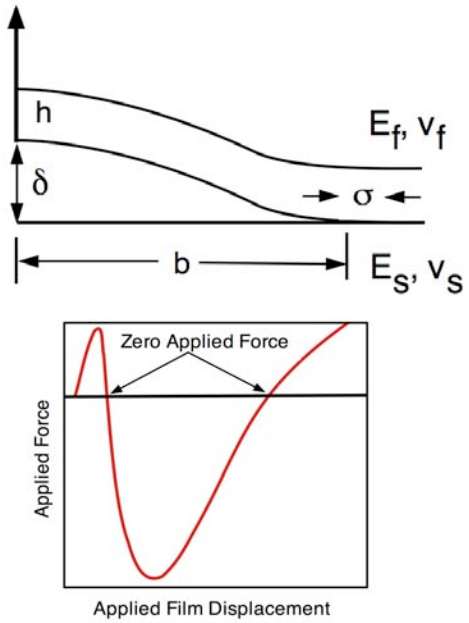

- Displace the center upwards
- Monitor the applied force
- When applied force equals zero, a free standing buckle exists

For W/PMMA,

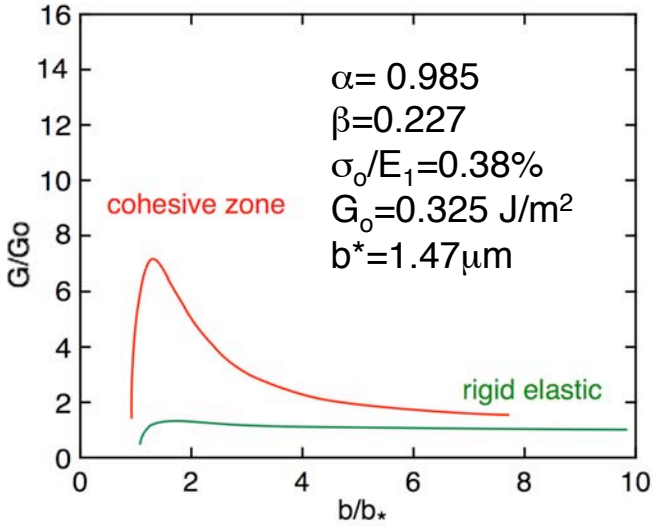

where,

$$b^* = \frac{\pi h}{2\sqrt{3}}\sqrt{\frac{E_f}{(1-\nu^2)\sigma}}$$

$$G_o = \sigma_o^2 h / 2\bar{E}$$

- The cohesive zone approach enables simulation of film performance in a component configuration

Cohesive Zone simulations compare well with the stress intensity based solutions from Yu and Hutchinson

.

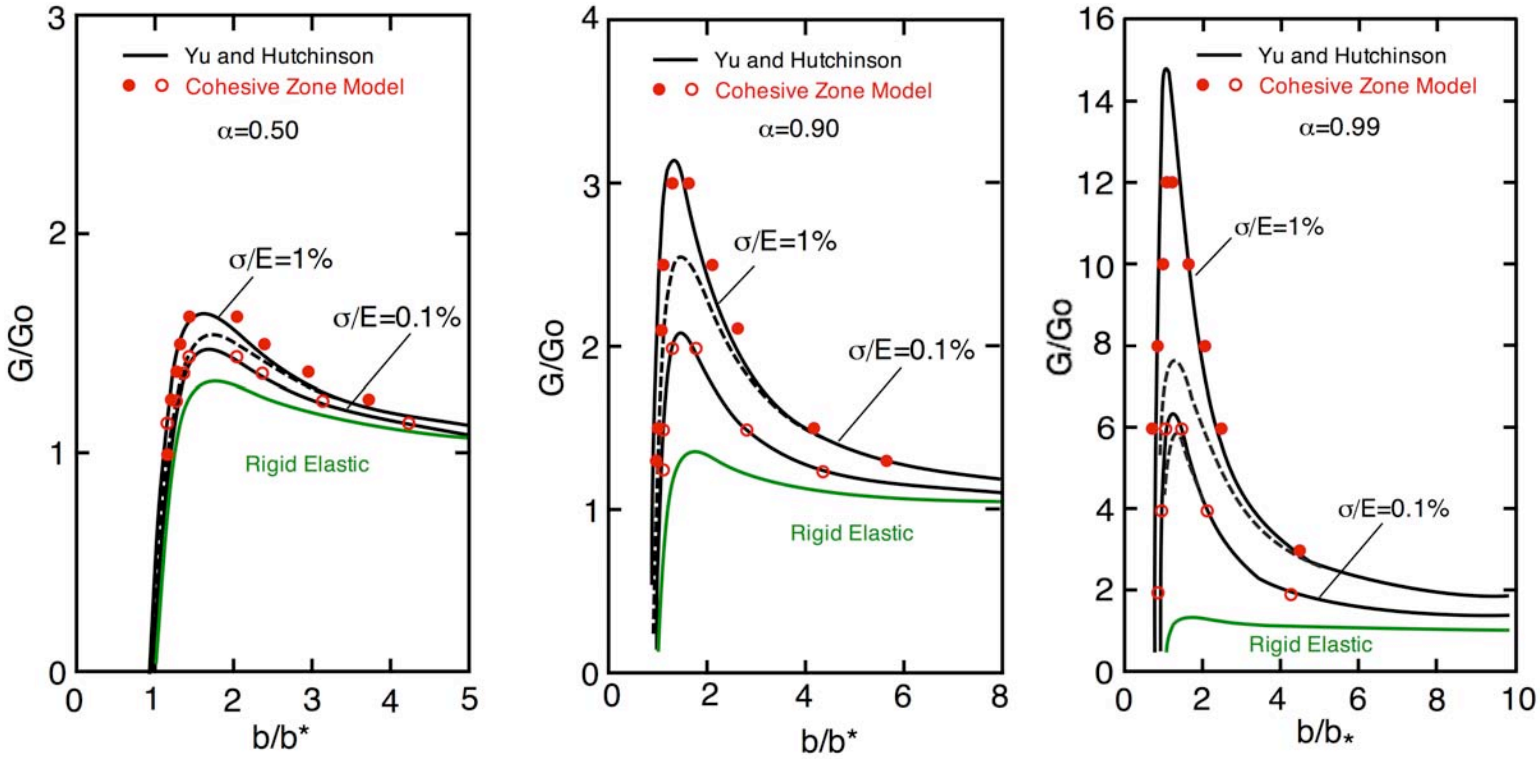

Substrate compliance had a significant effect on interfacial fracture energies that became very strong for small blisters and thick films.

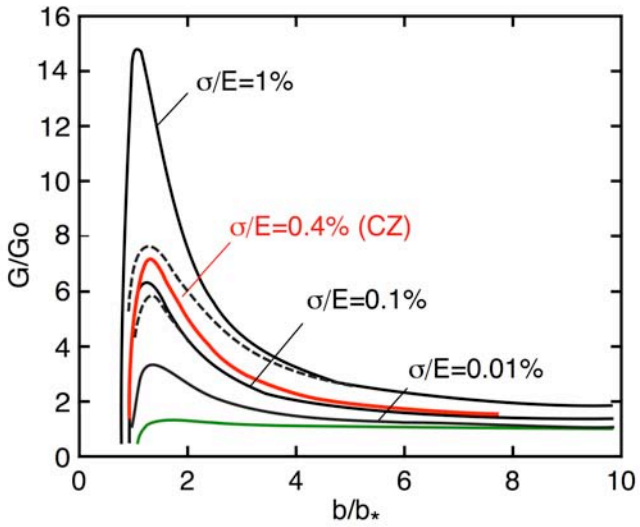

Rigid elastic and Cohesive Zone solutions were used to determine strain energy released.

The mode I contribution was defined as,

$$\Gamma_I = \Gamma(\psi) \Big/ \left[1 + \tan^2\{(1-\lambda)\psi\}\right]$$

with $\lambda = 0.3$

and ψ from the work of Suo and Hutchinson (1990) and Yu and Hutchinson (2005)

Buckles	Rigid Elastic			Cohesive Zone		
	$\Gamma(\psi)$ (J/m2)	ψ	Γ_I (J/m2)	$\Gamma(\psi)$ (J/m2)	ψ	Γ_I (J/m2)
100W/PMMA						
Small	0.4	-49	0.3	1.3	-49	0.9
Large	0.4	-75	0.2	0.6	-75	0.2
200W/PMMA						
Small	0.8	-39	0.6	4	-39	3.2
Large	0.7	-64	0.4	1.6	-64	0.8
400W/PMMA	1.5	-30	1.3	7.6	-30	6.5

Increasing substrate compliance dramatically alters the relationship between buckle morphology and stress

.

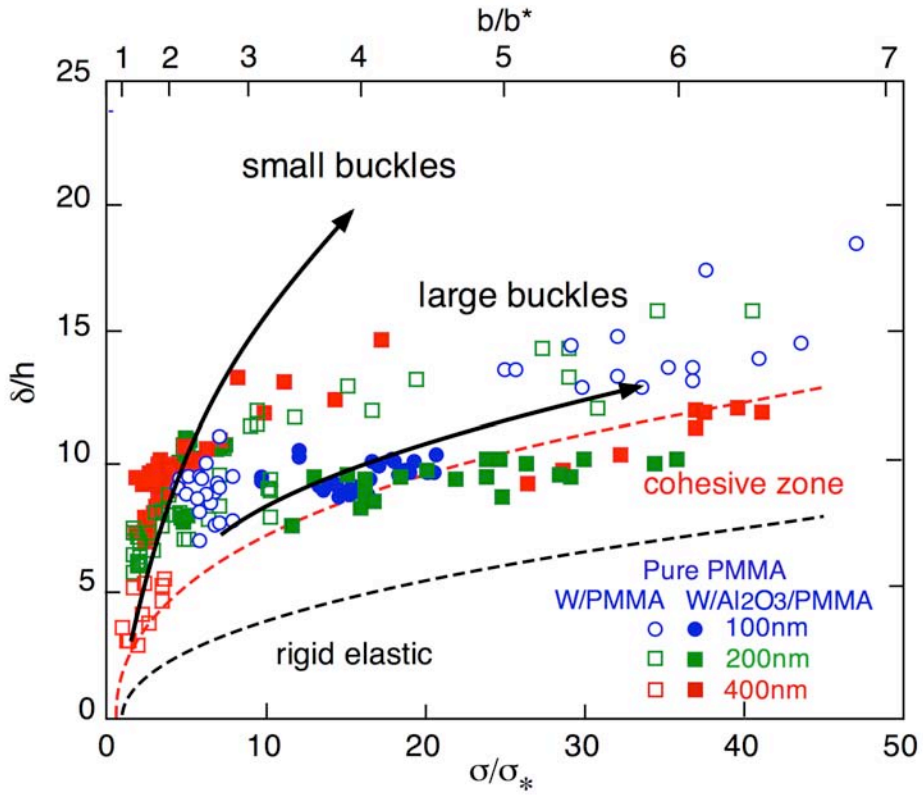

The results establish a lower bound to seemingly disparate data sets

The variance from linear elastic behavior indicates more than compliance is controlling behavior.

Buckle morphologies in a number of metal and ceramic film systems exhibit behavior close to rigid elastic prediction.

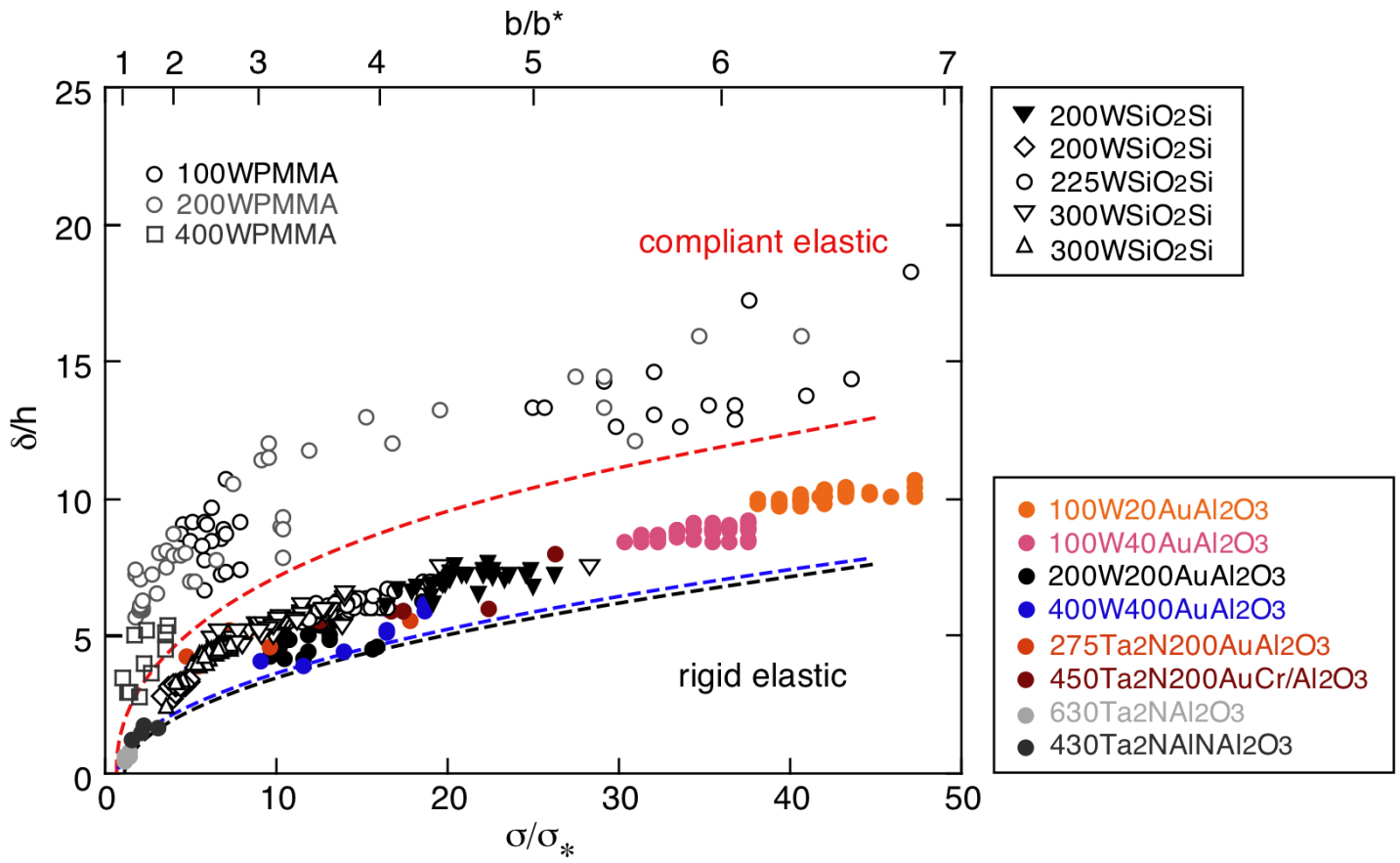

There is a common link – all buckles formed spontaneously.

Small buckle widths are three times smaller than those of the large buckles suggesting greater substrate deformation

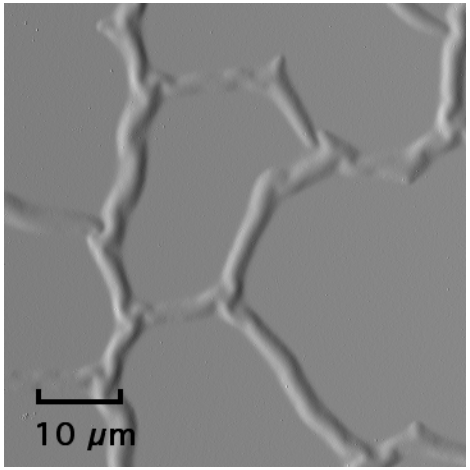

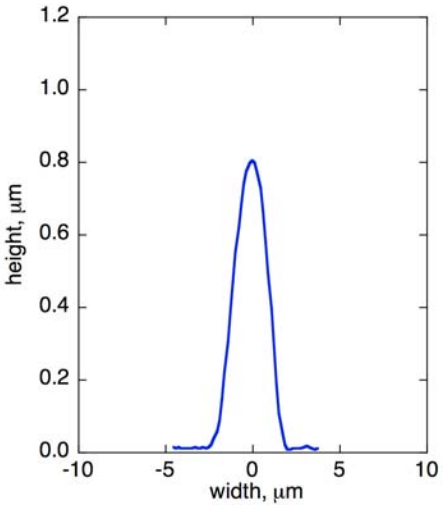

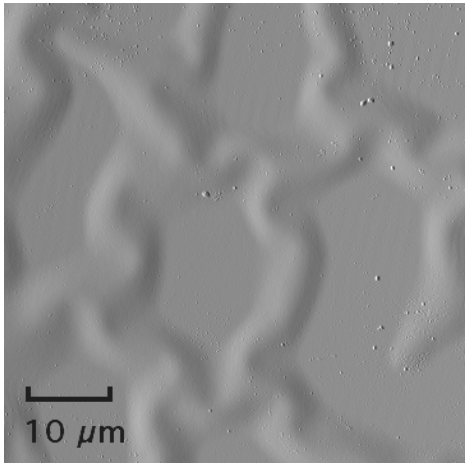

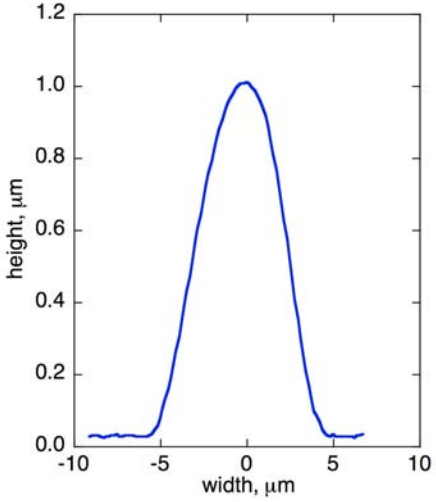

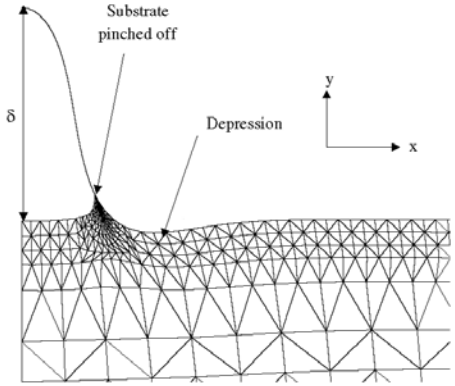

Parry and coworkers have shown that deformation leads to a 'meniscus' shape in a compliant substrate under the buckle

(Parry, Colin, Coupeau, Foucher, Cimetiere, Grilhe (2005)

The difference in buckle behavior may be due to differences in substrate deformation under large and small buckles

AFM indicates significant substrate deformation occurred in the PMMA substrates that extended well beyond buckle edges

small buckle

large buckle

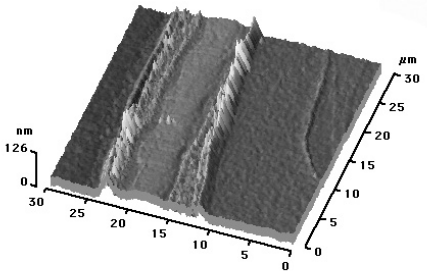

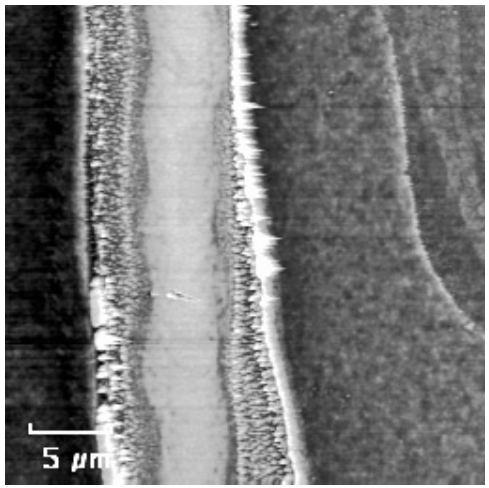

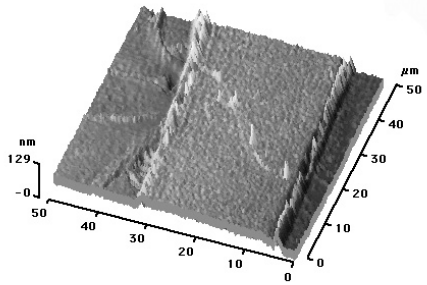

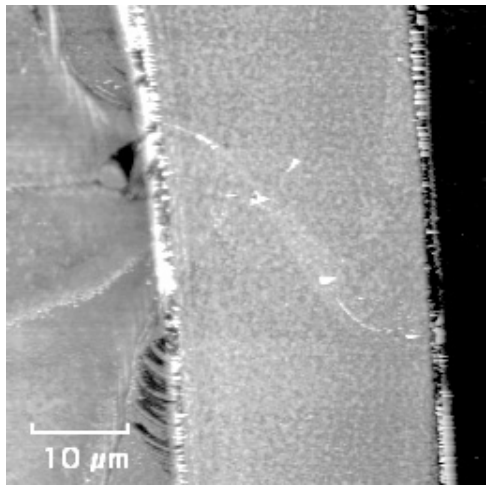

Increased substrate deformation along small buckle edges alters buckle morphology and increases fracture energies when compared to large buckles

Finite element simulations show that increasing shear leads to increased plasticity along a metal-polymer interface.

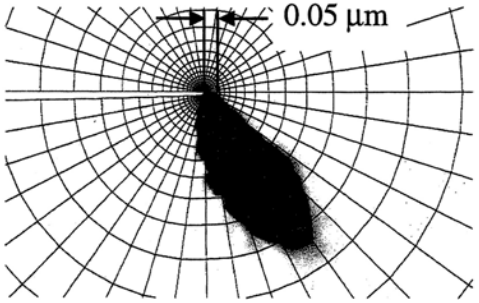

G=0.83 J/m^2
ψ=-22˚

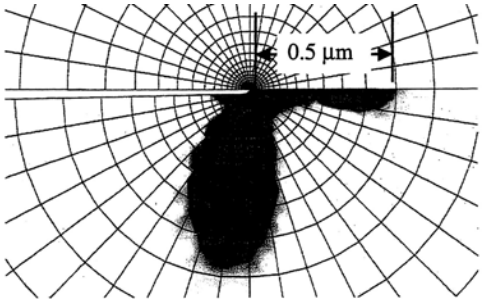

G=1.0 J/m^2
ψ=8˚

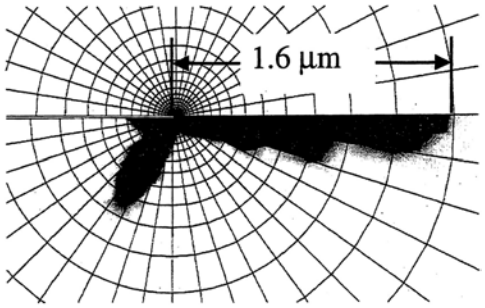

G=0.71 J/m^2
ψ=48˚

(E. D. Reedy, Jr.)

Plastic zone formation in W/PMMA follows behavior predicted for Si/Epon 828.

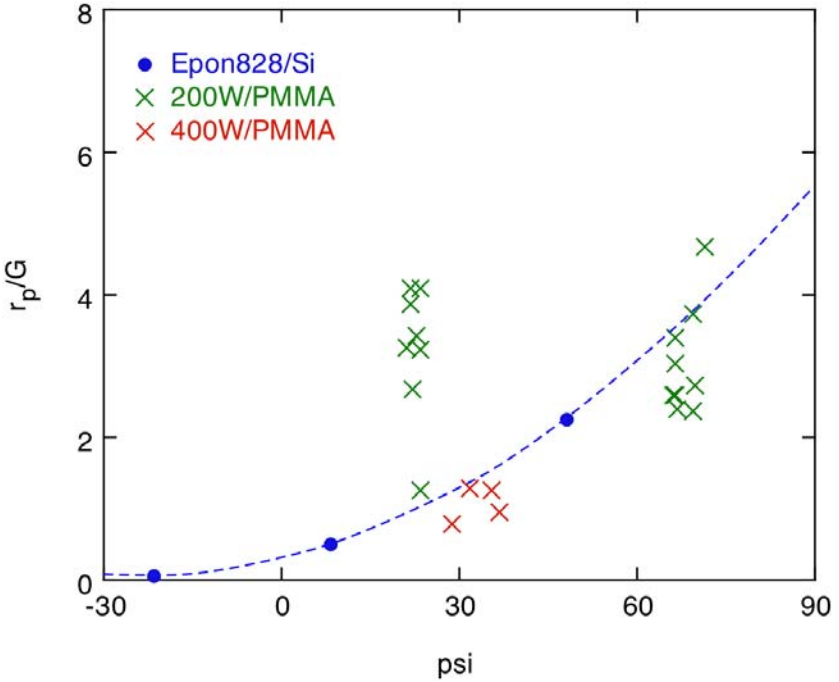

Rigid elastic buckle solutions for tungsten on PMMA

Substrate yielding occurs for all buckles forming on PMMA.

Finite element simulations show that increasing shear leads to increased plasticity along a metal-polymer interface.

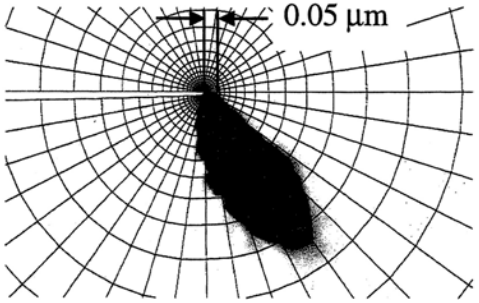

G=0.83 J/m^2
ψ=-22˚

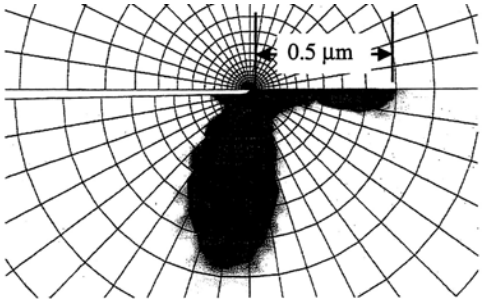

G=1.0 J/m^2
ψ=8˚

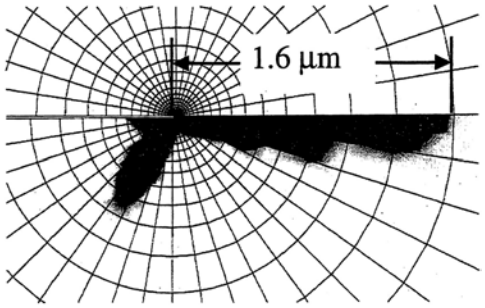

G=0.71 J/m^2
ψ=48˚

(E. D. Reedy, Jr.)

Plastic zone formation in W/PMMA follows behavior predicted for Si/Epon 828.

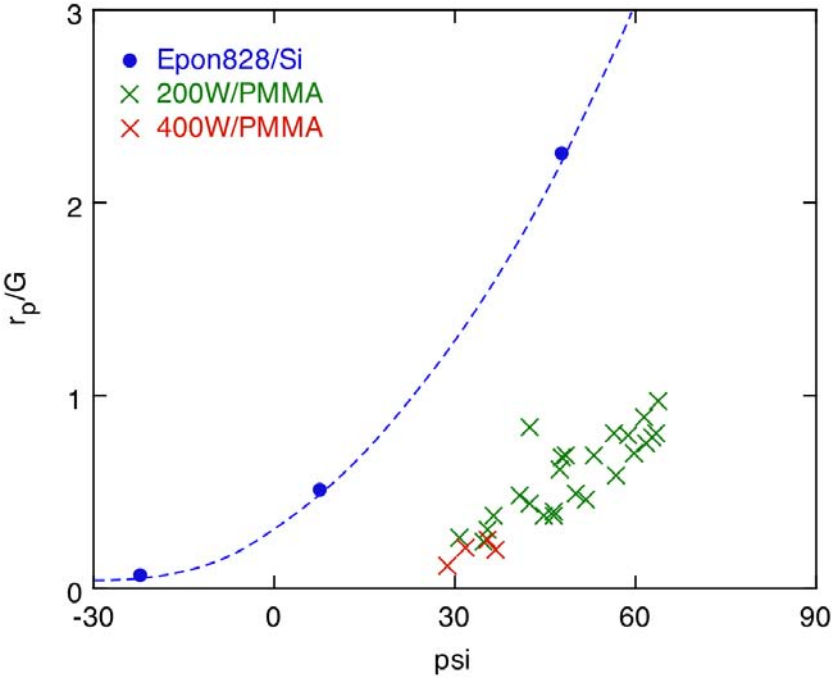

Cohesive Zone solutions for tungsten on PMMA

Results highlight the dramatic effects compliance has on crack behavior

The smallest buckles exhibited delamination, crack tip blunting, and substrate cracking.

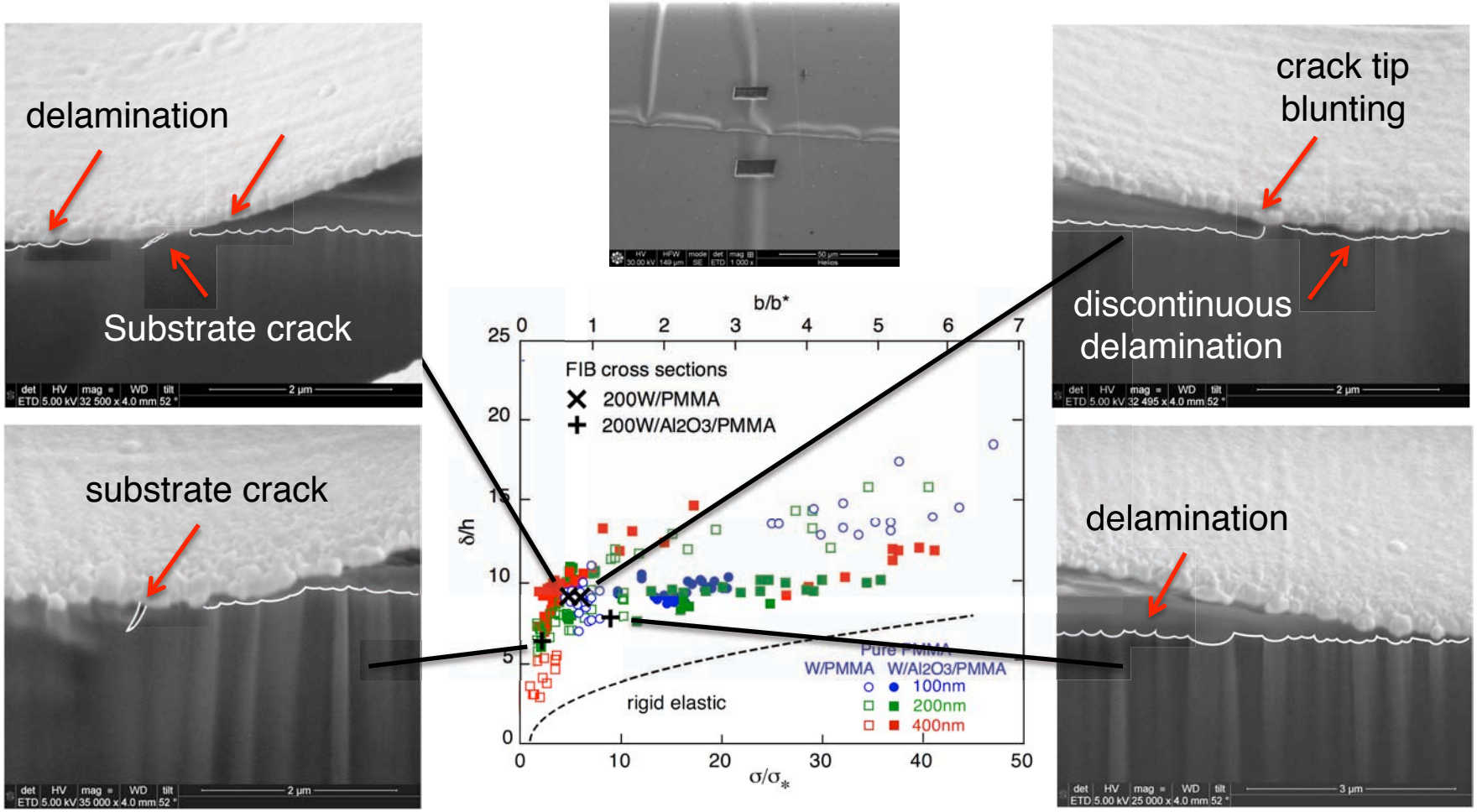

(D. Huber, J. E. Smugersky, H. L. Fraser)

The largest buckle failed by delamination.

The difference in behavior between large and small buckles correlates with localized plasticity in the PMMA substrate

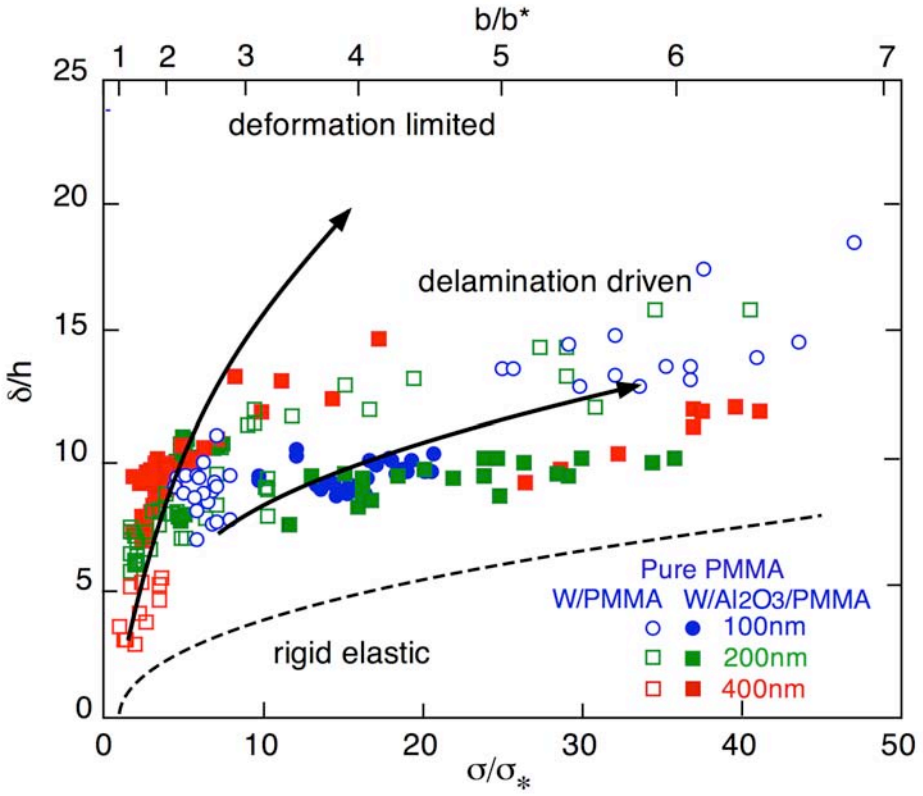

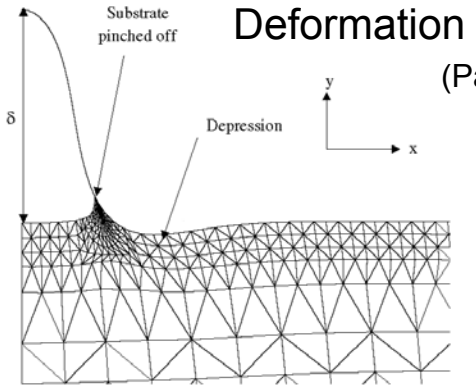

Deformation limited

(Parry et al.)

Delamination driven

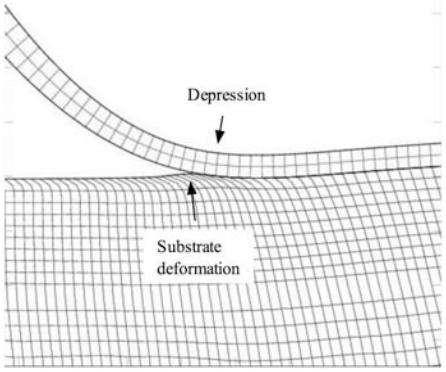

Simulations will need to include substrate yielding to accurately describe behavior.

Approach

Characterize deformation and fracture of thin ductile polymer films on copper coated substrates

Tasks

Spin 13, 100, 300 and 650 nm of PMMA onto copper coated silicon substrates. Deposit a tungsten overlayer to stress the thin PMMA films.

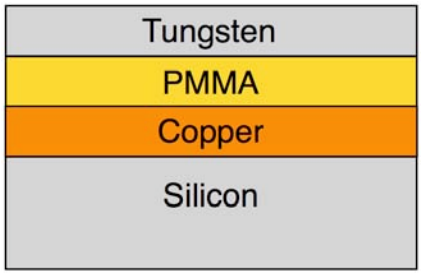

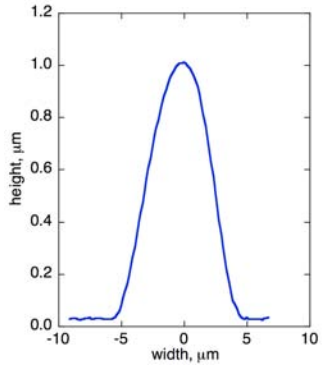

Used optical and atomic force microscopy to characterize film buckling and substrate deformation.

Determined interfacial fracture energies from models describing effects of substrate compliance and deformation on fracture

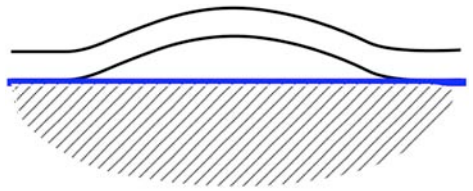

Buckles formed following deposition of tungsten on thin PMMA Films

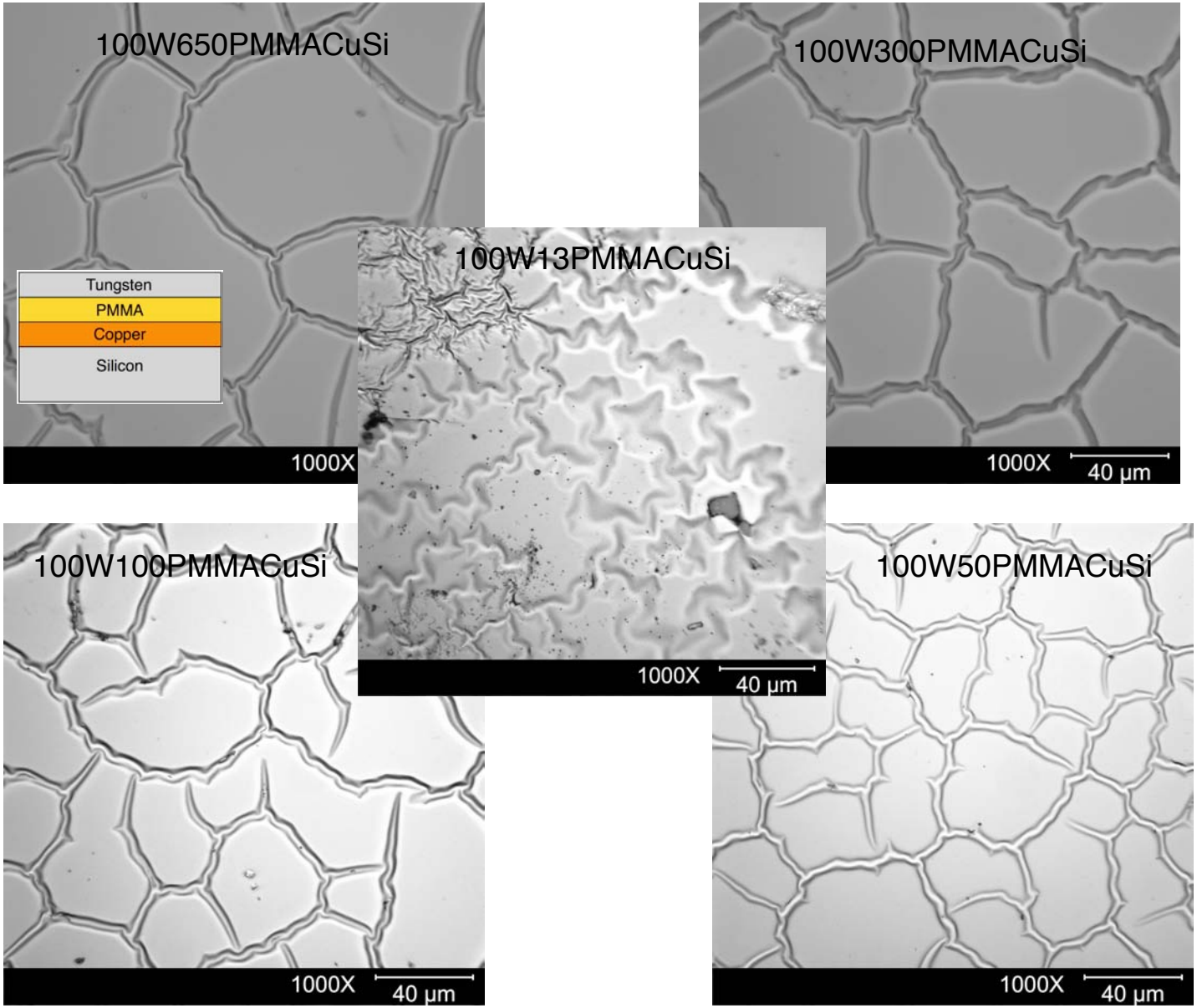

Substrate compliance also had a significant effect on thin PMMA films.

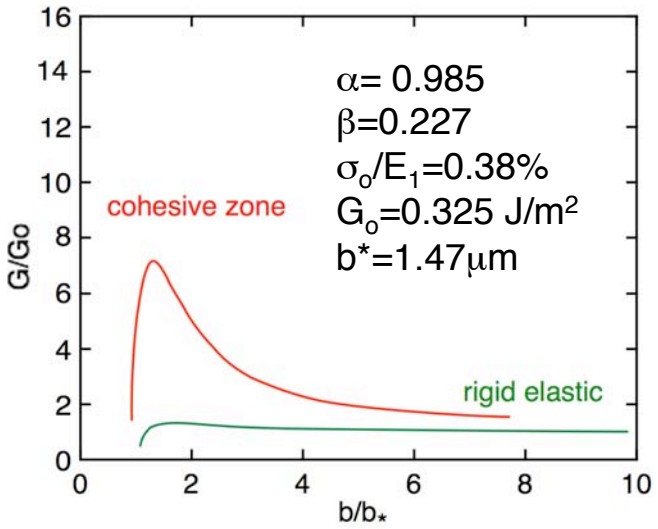

Rigid elastic and Cohesive Zone solutions were used to determine strain energy released.

The mode I contribution was defined as,

$$\Gamma_I = \Gamma(\psi) \Big/ \left[1 + \tan^2\{(1-\lambda)\psi\}\right]$$

with $\lambda = 0.3$

and ψ from the work of Suo and Hutchinson (1990) and Yu and Hutchinson (2005)

Buckles	Rigid Elastic			Cohesive Zone		
	$\Gamma(\psi)$ (J/m2)	ψ	Γ_I (J/m2)	$\Gamma(\psi)$ (J/m2)	ψ	Γ_I (J/m2)
100W/650PMMA	0.5	-55	0.3	1.4	-55	0.9
100W/300PMMA	0.5	-55	0.3	1.5	-55	0.9
100W/100PMMA	0.5	-51	0.3	1.7	-51	1.1
100W/50PMMA	0.5	-58	0.3	1.3	-58	0.8
100W/13PMMA	0.5	-72	0.2	0.8	-72	0.3

A transition in substrate effects occurs when PMMA film thickness becomes less than the thickness of the tungsten overlayer

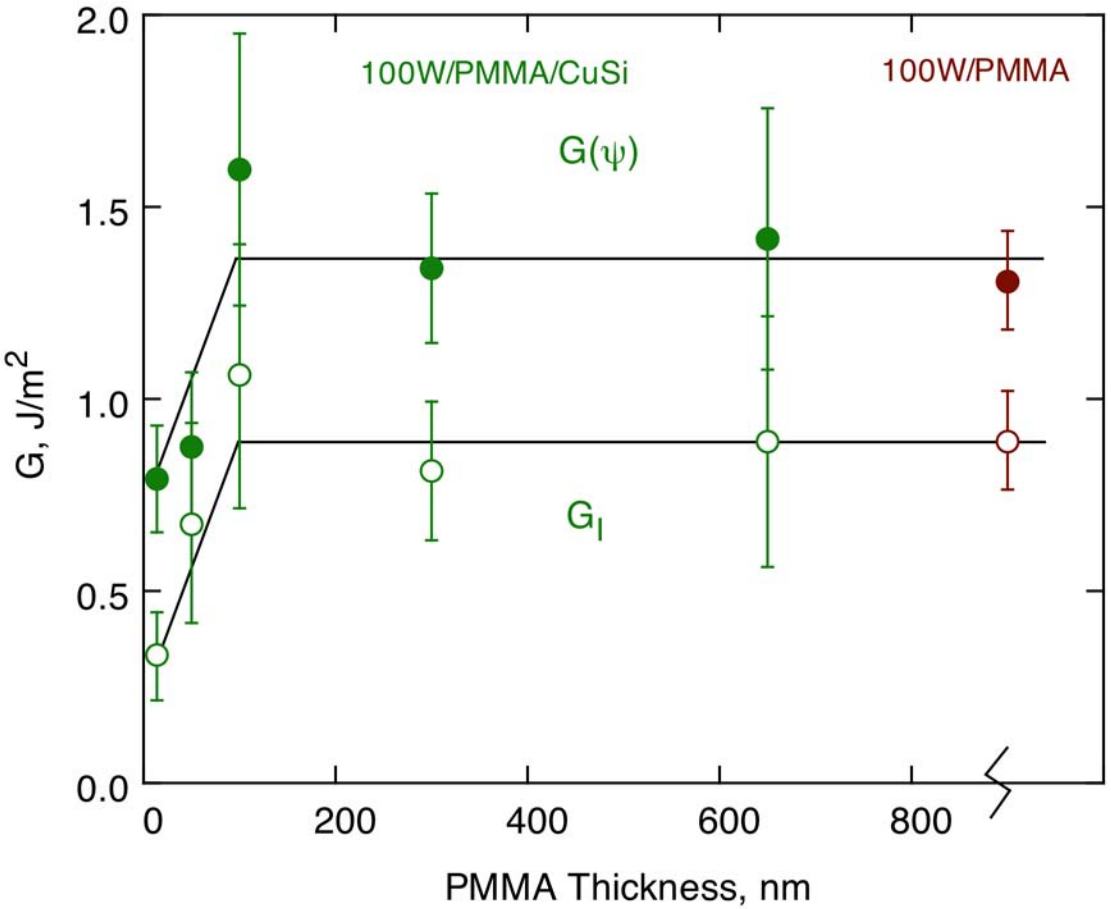

PMMA continues to exert a strong effect even when several times thinner than the metal overlayer thickness

For thick films, the mode I energies are similar to mode I toughness values from indentation testing

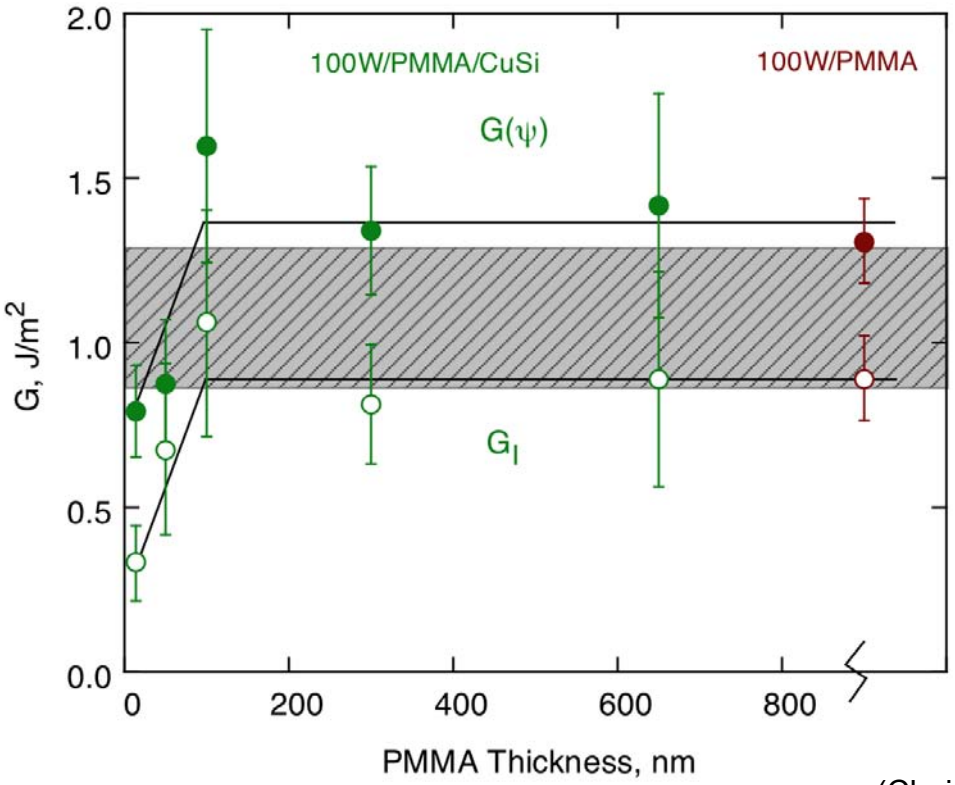

G_{Ic} ~ 1.1 J/m^2

(Choi and Salem)

A transition from compliant elastic to rigid elastic behavior occurs as PMMA film thickness decreases.

.

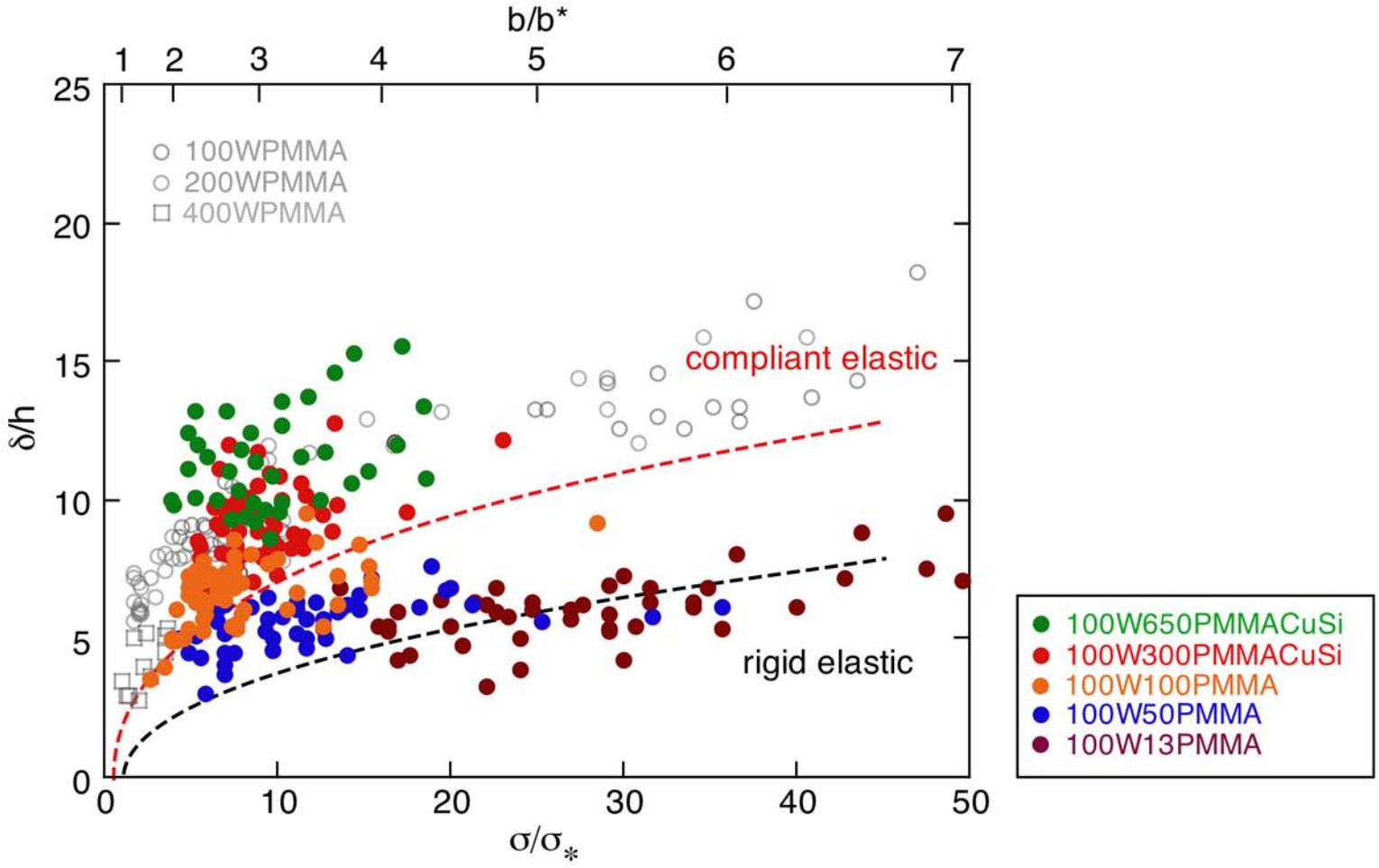

The 13 nm thick PMMA film system exhibits rigid elastic behavior.

A transition from compliant elastic to rigid elastic behavior occurs as PMMA film thickness decreases.

.

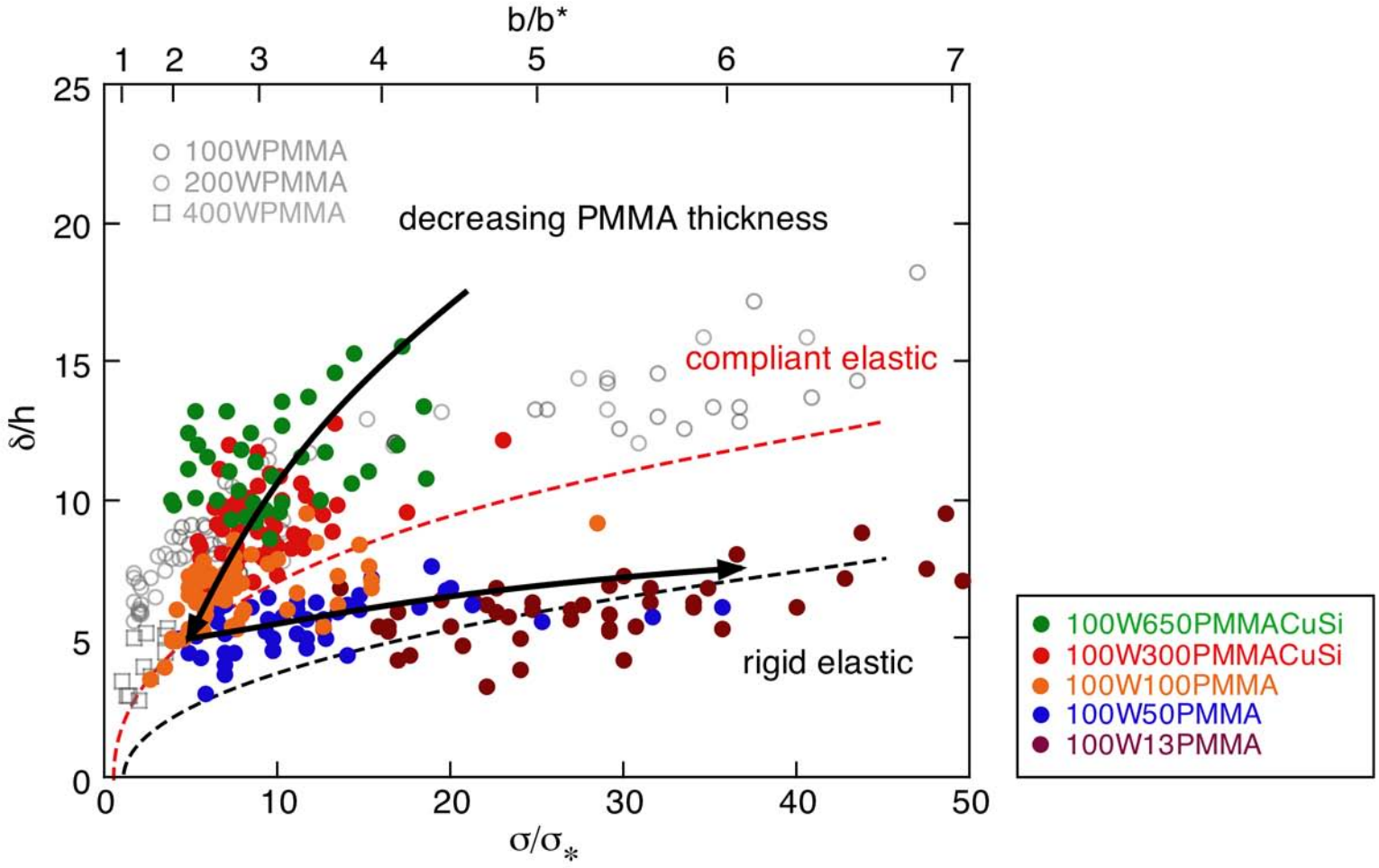

The 13 nm thick PMMA film system exhibits rigid elastic behavior.

Intense river markings indicate deformation occurred in all but the thinnest PMMA film.

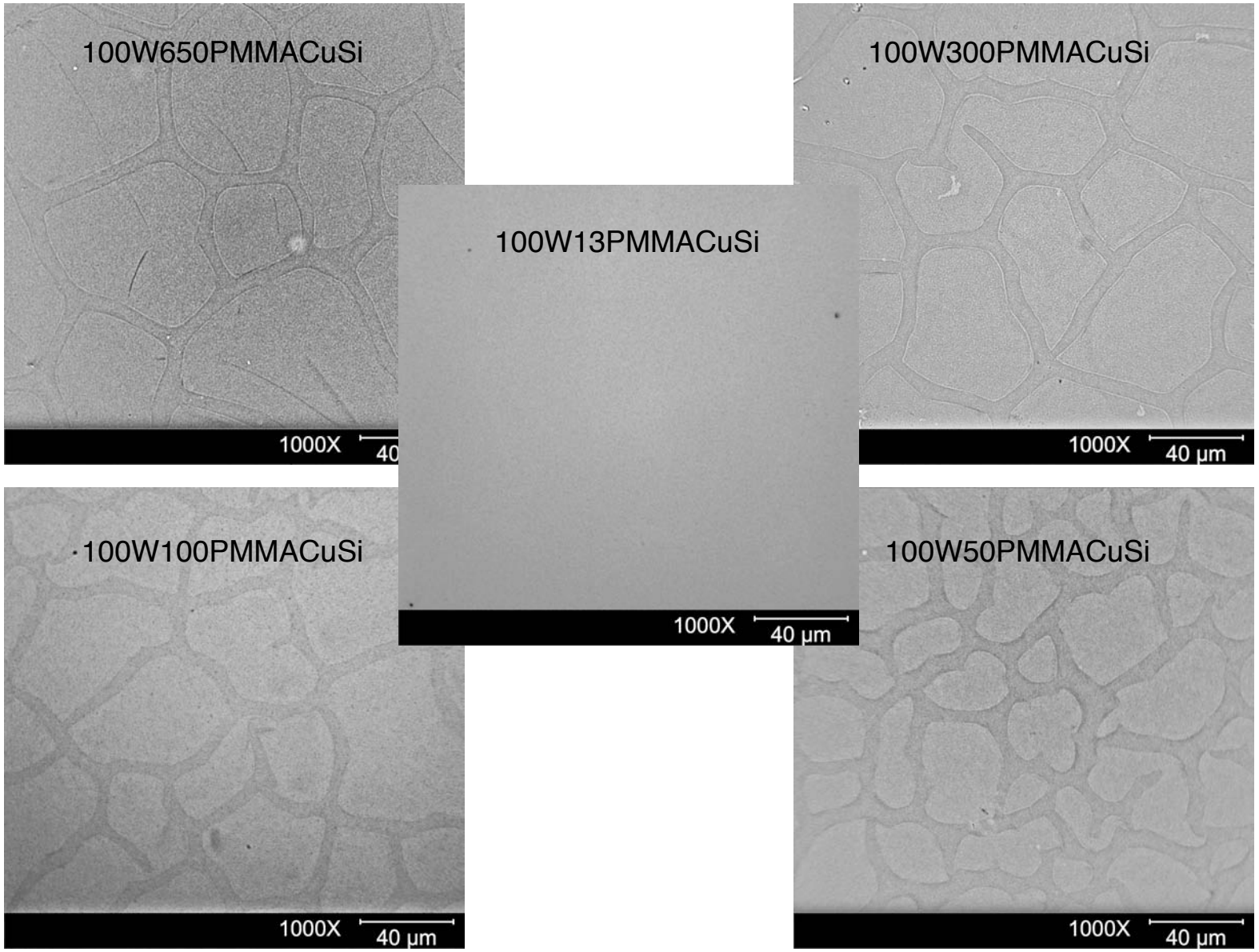

Finite element simulations show that increasing shear leads to increased plasticity along a metal-polymer interface.

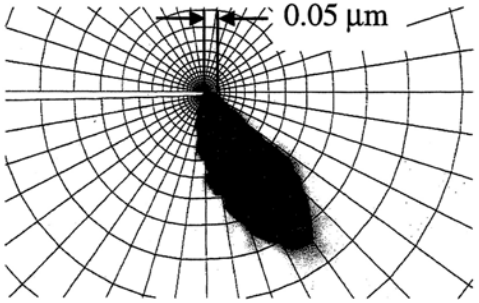

G=0.83 J/m^2
ψ=-22˚

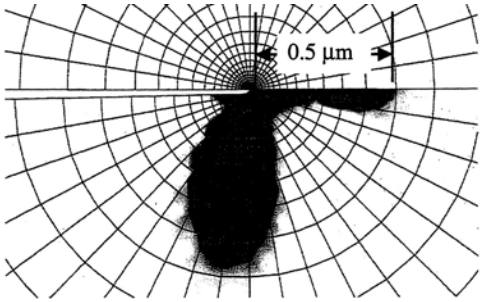

G=1.0 J/m^2
ψ=8˚

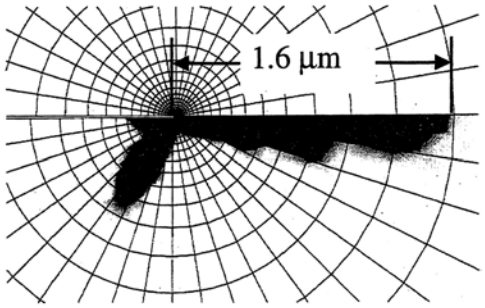

G=0.71 J/m^2
ψ=48˚

(E. D. Reedy, Jr.)

Plastic zone formation in W/PMMA follows behavior predicted for Si/Epon 828.

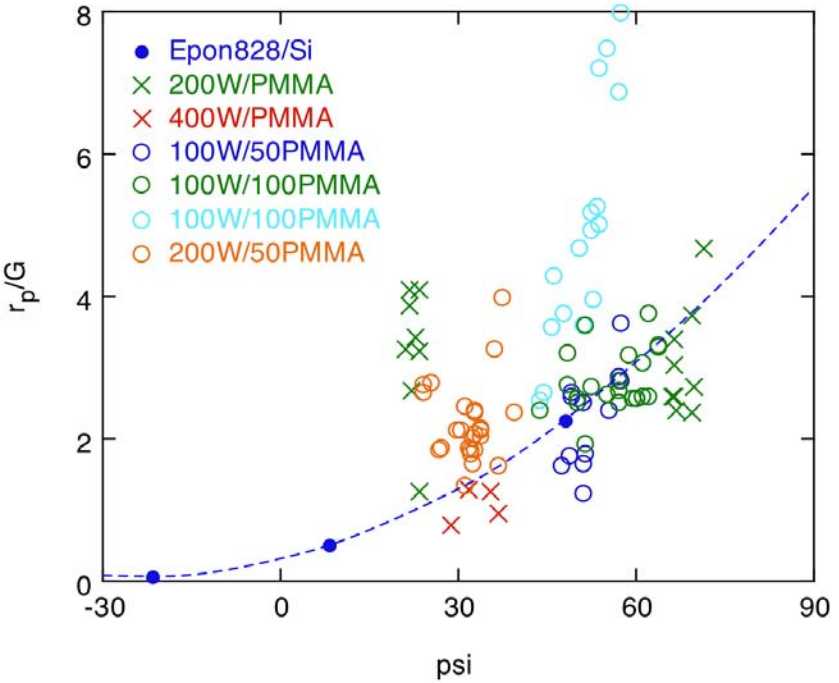

Rigid elastic buckle solutions for tungsten on PMMA

Substrate yielding occurs for all buckles forming on PMMA.

Finite element simulations show that increasing shear leads to increased plasticity along a metal-polymer interface.

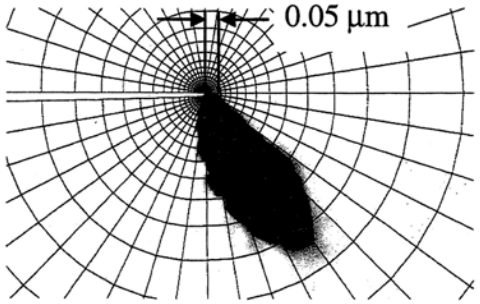

G=0.83 J/m^2
ψ=-22˚

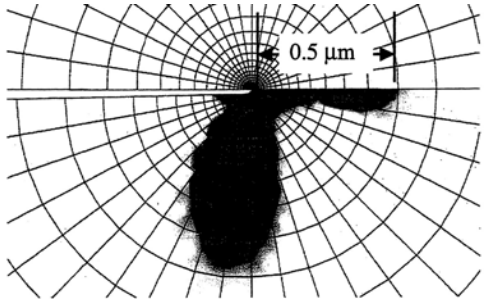

G=1.0 J/m^2
ψ=8˚

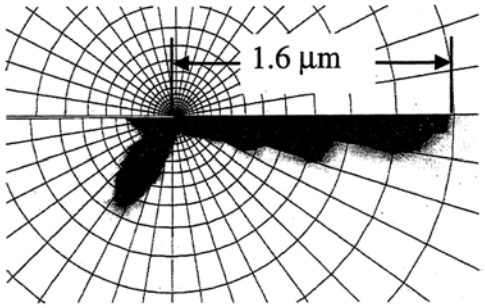

G=0.71 J/m^2
ψ=48˚

(E. D. Reedy, Jr.)

Plastic zone formation in W/PMMA follows behavior predicted for Si/Epon 828.

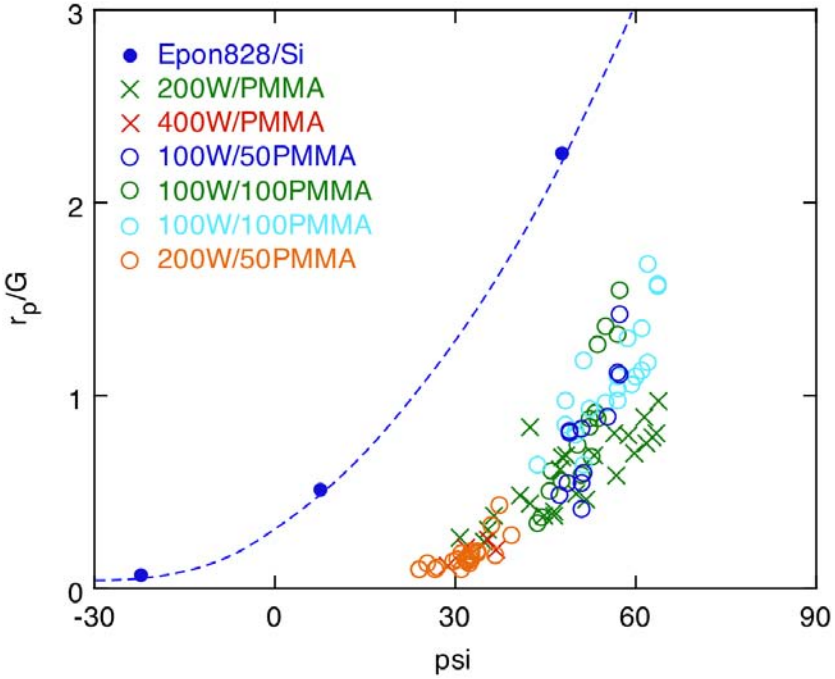

Cohesive Zone solutions for tungsten on PMMA

Results highlight the dramatic effects compliance has on crack behavior

XPS and AES analyses indicate that PMMA remains on the substrate surface after tungsten film delamination from the 13nm PMMA sample

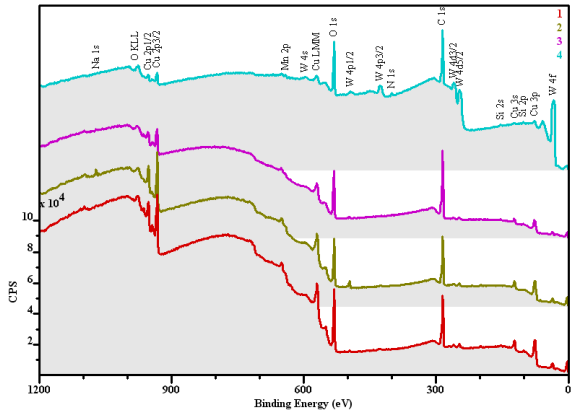

Traces 1-3 and the shape of the background signal indicate the presence of PMMA.

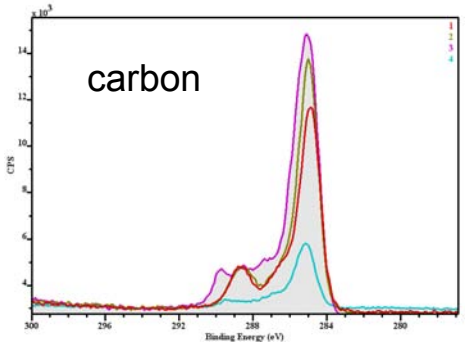

The structure of the carbon signal and the line shape indicate PMMA on the surface.

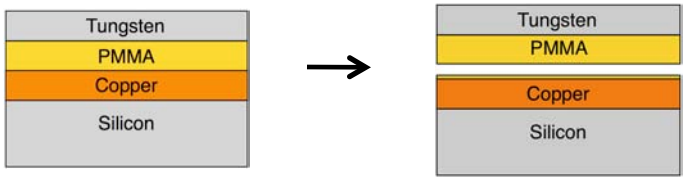

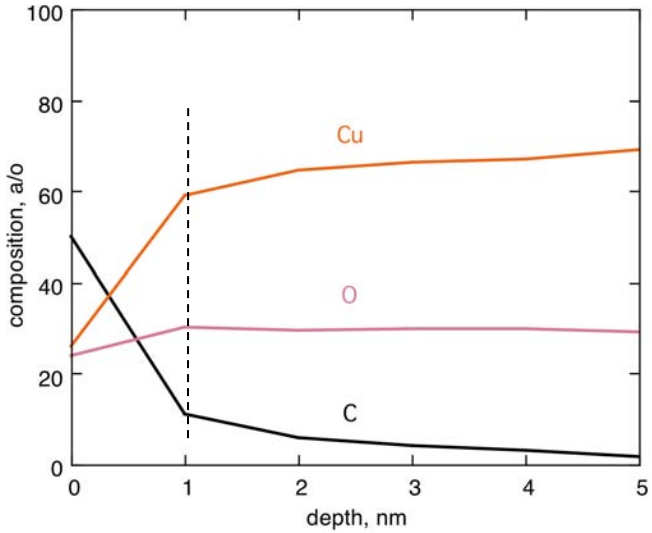

AES indicates a very thin layer of PMMA remains on the copper coated substrate surface

(M. Brumbach, W. Wallace, M. Clift)

SAM and XPS show fracture in all samples occurs in the PMMA film.

.

Significant changes in properties can extend more than 25 nm from the surface and 100 nm from the interface

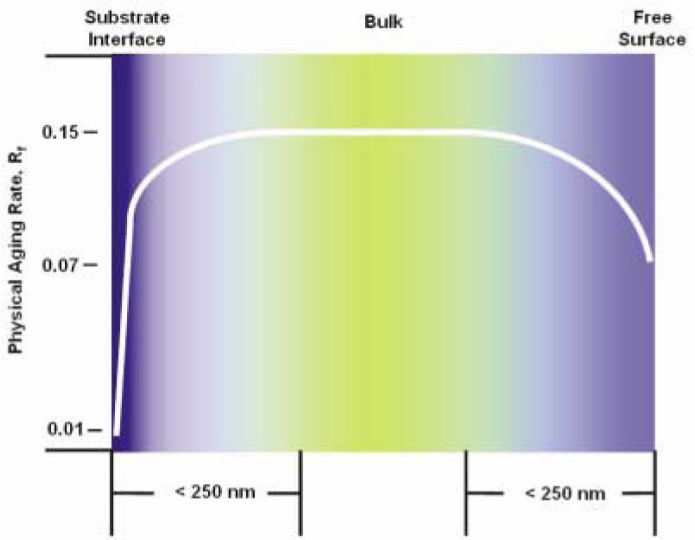

(Priestly et al. Science 2005)

For films thicker than 100 nm, fracture occurred near the tungsten overlayer

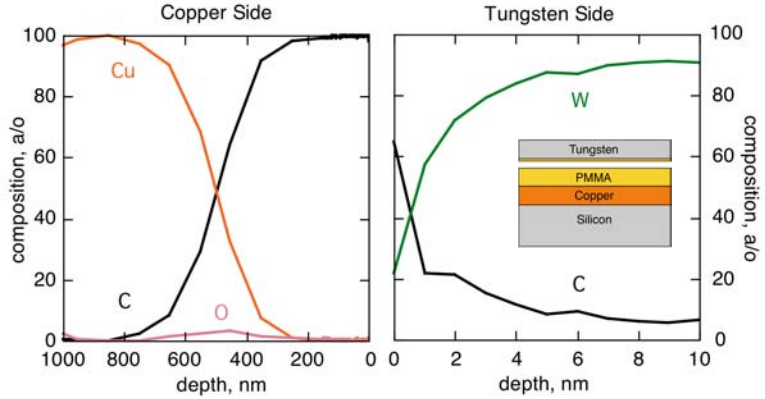

For the 13 nm thick film, fracture occurred near the copper coated substrate

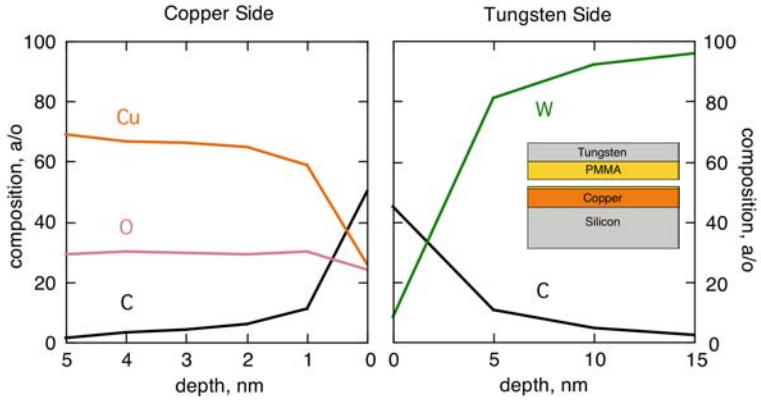

The film properties measured are not the properties that affect fracture.

Four point bend fracture tests provide an another method for measuring of polymer-metal interfacial fracture energies

.

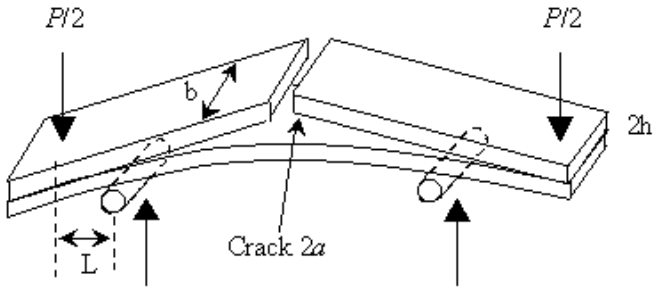

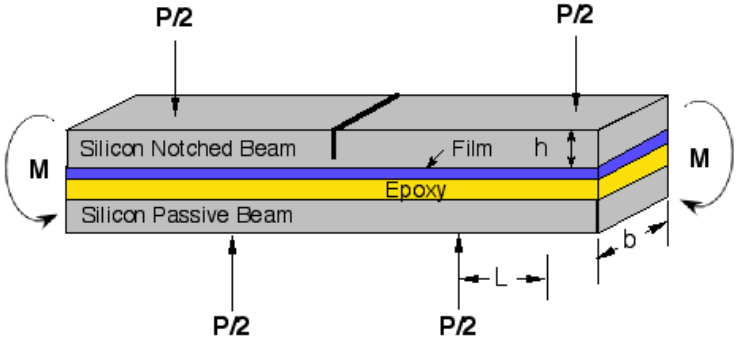

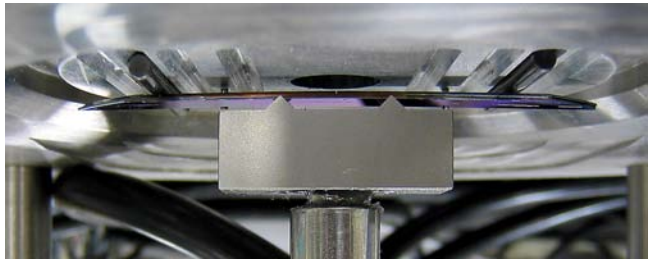

Samples were designed to to focus crack growth along the Cu/PMMA interface.

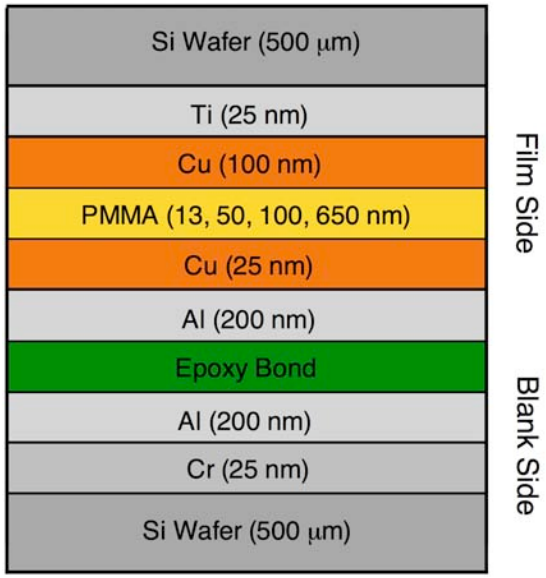

(M. Ong)

Plateaus in the load-displacement curves define the critical loads for stable crack growth and values for calculating fracture energies

.

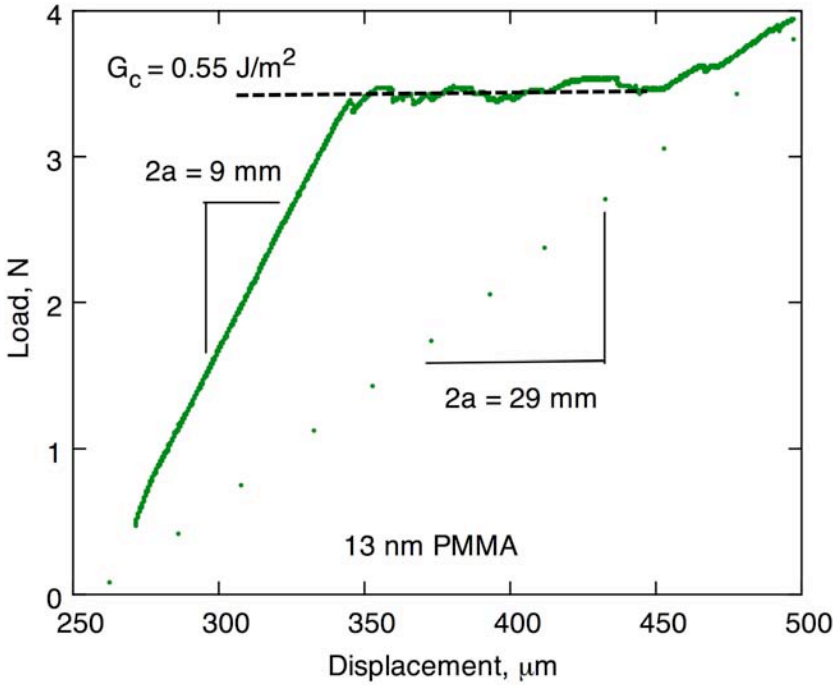

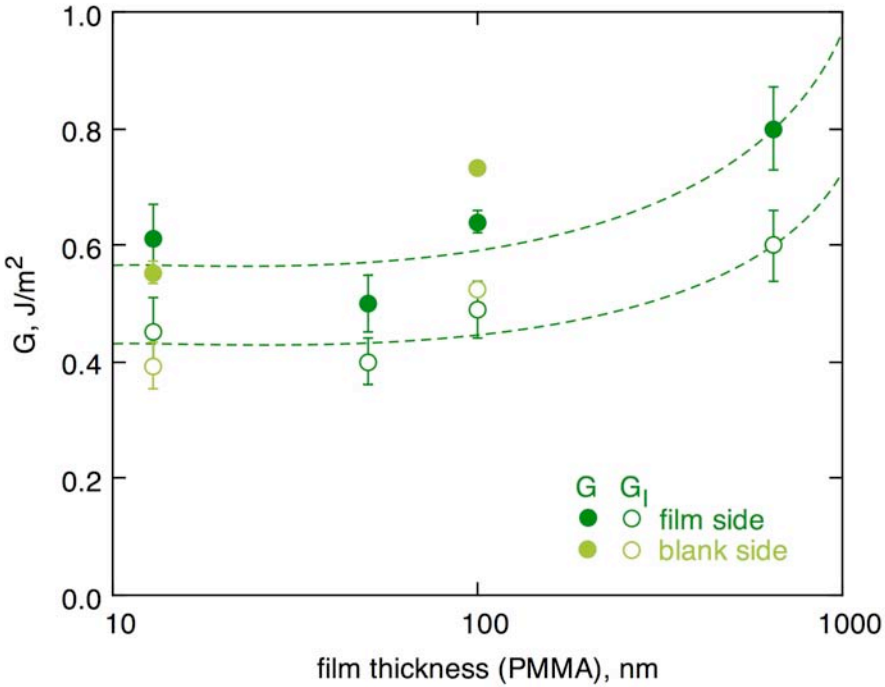

Fracture Energy

$$\Gamma(\psi) = \frac{21P^2L^2\left(1-\nu^2\right)}{16Eb^2h^3}$$

Practical Work of Adhesion

$$\Gamma_I = \Gamma(\psi)\Big/\left[1+\tan^2\left\{(1-\lambda)\psi\right\}\right]$$

$$\lambda = 0.3, \psi = 43^\circ$$

(M. Ong)

Fracture energies are similar to those measured using stressed overlayers.

AES shows that fracture in all samples occurred within the PMMA film

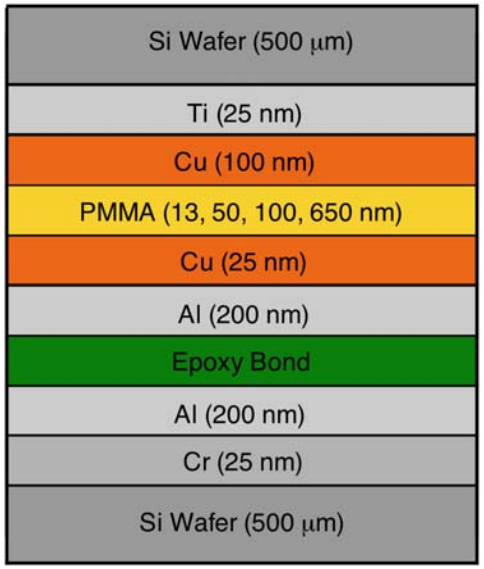

100 nm PMMA

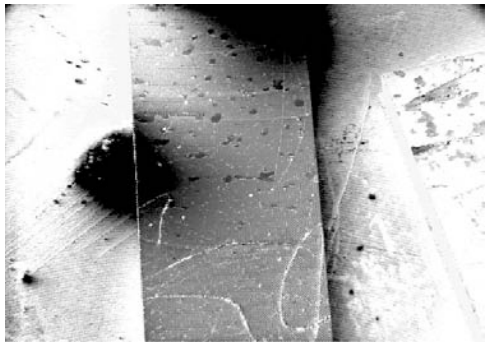

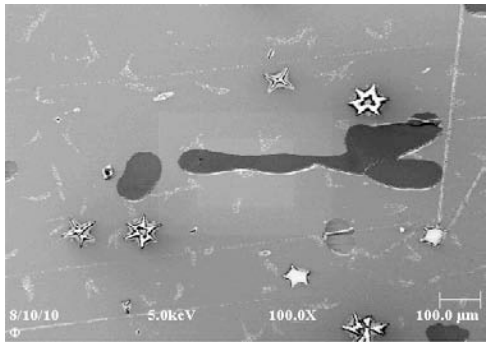

Sample	Side Analyzed	C	O	Cu	Al
650 PMMA	Notch	97.0	3.0		
650 PMMA	Op-Notch	67.4	12.3	18.6	
100 PMMA	Notch	93.0	5.0		
100 PMMA	OP-Notch	81.5	5.3		11.4
50 PMMA	Notch	86.8	4.1	9.1	
50 PMMA	OP-Notch	87.4	4.3	2.2	6.3
13 PMMA	Notch	69.6	10.1	19.7	
13 PMMA	OP-Notch	56.2	16.7	5.7	21.2

(M. Ong)

Summary

- Buckles formed spontaneously on W-PMMA film systems creating relatively uniform patterns of buckles
- In polymer-metal systems, increasing substrate compliance led to significantly higher interfacial fracture energies than indicated by a rigid substrate analysis
- Failure in polymer-metal systems parallel the gradients in polymer properties created by changes in structural relaxation rates

The results show that buckles exhibit rigid elastic behavior only when films are significantly thinner than the stressed tungsten overlayer.

Acknowledgments

.

The support of Sandia National Laboratories is gratefully acknowledged.

Sandia is a multiprogram laboratory operated by Sandia Corporation, a Lockheed Martin Company for the United States Department of Energy's National Nuclear Security Administration under contract DE-AC04-94AL85000

Traditional Test Techniques

DCB Sample

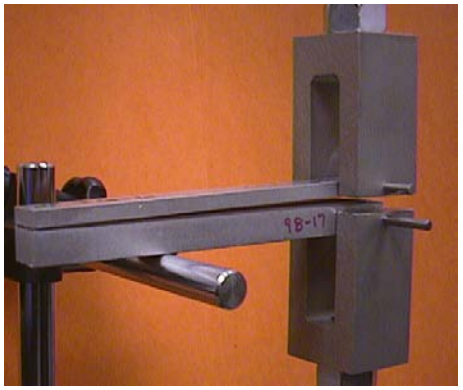

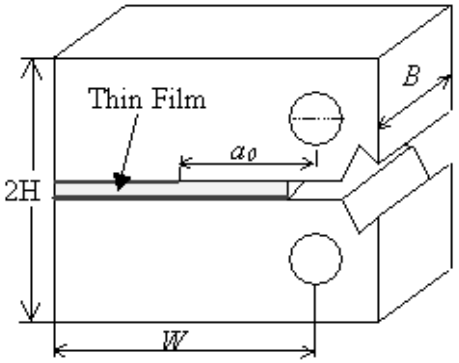

K_{Ic} CTS

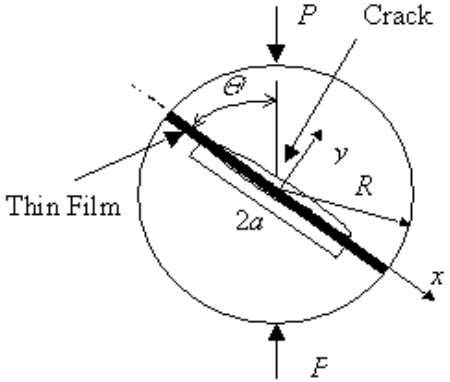

Brazil Nut Sample

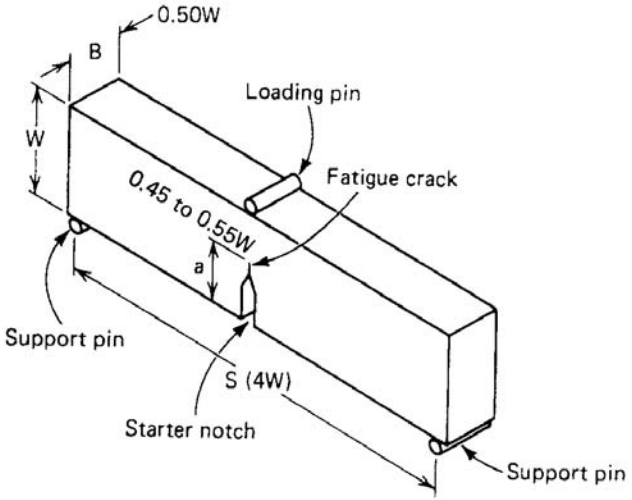

Bend Sample

These are material intensive tests where fabrication may alter film and interface structure and composition

Thin Film Test Techniques

Interfacial fracture of hard thin elastic films is readily studied using stressed overlayer, nanoindentation, and nanoscratch tests.

---

uniform width blisters

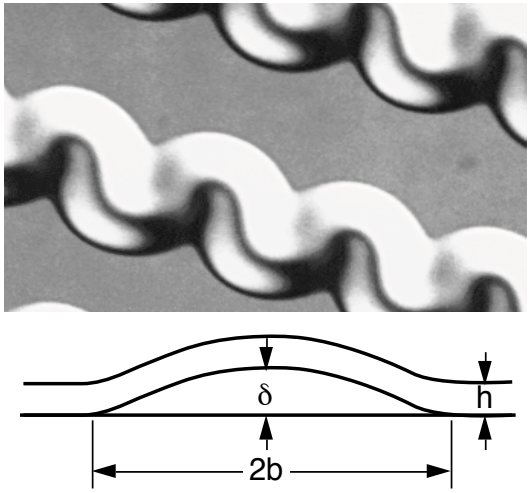

nanoindentation blisters

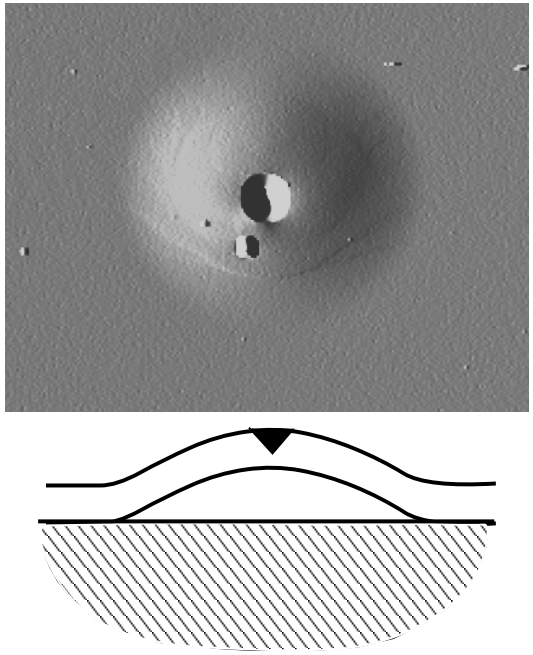

nanoscratch blisters

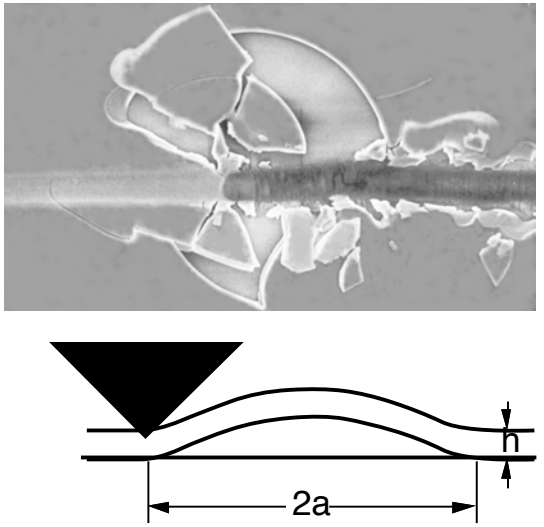

The techniques can be extended to the study of thin ductile films